Vortex statistics in a disordered two-dimensional *XY* model

Lei-Han Tang
Institut für Theoretische Physik, Universität zu Köln, Zülpicher Strasse 77, D-50937 Köln, Germany
and Condensed Matter Theory, The Blackett Laboratory, Imperial College, London SW7 2BZ, United Kingdom
(Received 15 February 1996; revised manuscript received 12 April 1996)

The equilibrium behavior of vortices in a classical two-dimensional (2D) *XY* model with uncorrelated random phase shifts is investigated. The model describes Josephson-junction arrays with positional disorder and has ramifications in a number of other bond-disordered 2D systems. The vortex Hamiltonian is that of a Coulomb gas in a background of quenched random dipoles, which is capable of forming either a dielectric insulator or a plasma. We confirm a recent suggestion by Nattermann, Scheidl, Korshunov, and Li [J. Phys. (France) I **5**, 565 (1995)] and by Cha and Fertig [Phys. Rev. Lett. **74**, 4867 (1995)] that, when the variance σ of random phase shifts is sufficiently small, the system is in a phase with quasi-long-range order at low temperatures, without a reentrance transition. This conclusion is reached through a nearly exact calculation of the single-vortex free energy and a Kosterlitz-type renormalization group analysis of screening and random polarization effects from vortex-antivortex pairs. There is a critical disorder strength σ_c, above which the system is in the paramagnetic phase at any nonzero temperature. The value of σ_c is found not to be universal, but generally lies in the range $0<\sigma_c<\pi/8$. In the ordered phase, vortex pairs undergo a series of spatial and angular localization processes as the temperature is lowered. This behavior, which is common to many glass-forming systems, can be quantified through approximate mappings to the random energy model and to the directed polymer on the Cayley tree. Various critical properties at the order-disorder transition are calculated. [S0163-1829(96)06329-1]

I. INTRODUCTION

The Kosterlitz-Thouless-Berezinskii (KTB) transition[1–3] plays an important role in the theory of ordering in two-dimensional (2D) systems which have a continuous symmetry specified by a phase. Examples include planar magnets, 2D solids, Josephson-junction arrays, superfluid and superconductor films, etc.[4] These systems have an ordered phase at low temperatures, characterized by a power-law decay of correlations with distance. The (quasi-) long-range order is destroyed through unbinding of vortex-antivortex pairs, which takes place at the KTB transition.

A question of both theoretical and practical interest is whether and how quenched disorder alters the above picture. In this paper we shall focus on the case of random frustration, where disorder introduces random, uncorrelated phase shifts but does not pin the phase angles themselves. More precisely, we shall consider an *XY* model with the Hamiltonian[5]

$$H(\{\phi_i\})=-J\sum_{\langle ij\rangle}\cos(\phi_i-\phi_j-A_{ij}), \tag{1.1}$$

where the sum runs over all nearest-neighbor pairs on a square lattice. The quenched random variables A_{ij}, which give a random bias to the preferred advancing angle over each bond, are assumed to be uncorrelated from bond to bond, and each is Gaussian distributed with the mean and variance given by

$$\langle A_{ij}\rangle=0, \quad \langle A_{ij}^2\rangle=\sigma, \tag{1.2}$$

respectively. It has been suggested that model (1.1) provides a good description of the Josephson-junction arrays in a transverse magnetic field.[6–10] In this case, ϕ_i is identified with the phase of the superconducting order parameter of grain i, and $A_{ij}=(2\pi/\Phi_0)\int_{i\to j}\mathbf{A}_{\rm ext}\cdot d\mathbf{l}$, where $\mathbf{A}_{\rm ext}$ is the vector potential of the external magnetic field and $\Phi_0=hc/2e$ is the superconducting flux quantum. The case (1.2) corresponds to a situation where the average magnetic flux over each elementary plaquette of the grain network is an integer multiple of Φ_0, but random displacement of superconducting grains from a perfect lattice structure yields quenched random phase shifts.[7,11]

On the theoretical side, model (1.1) and its variants have been studied extensively in the past.[5,12–20] Result of previous studies can be summarized as follows. (i) The spin-wave fluctuations have essentially the same excitation spectrum as in the pure case. Disorder introduces distortion in the ground state away from a perfect ferromagnetic alignment. The combined effect of thermal and disorder fluctuations leads to an algebraic decay of the two-point phase-phase correlation function

$$C_{\rm sw}(r_{ij})\equiv\langle\exp[i(\phi_{{\rm sw},i}-\phi_{{\rm sw},j})]\rangle\sim r_{ij}^{-\eta_{\rm sw}}, \tag{1.3}$$

where r_{ij} is the distance between site i and j, and

$$\eta_{\rm sw}=\frac{1}{2\pi}\left(\frac{T}{J}+\sigma\right) \tag{1.4}$$

is the correlation length exponent at temperature T, due to spin waves only. (ii) Vortices, which are topological point defects in the ϕ field, interact with each other and with the quenched disorder through a Coulomb potential. The interaction between two vortices is of the charge-charge type, where the charge of each vortex is given by its vorticity. The interaction between a vortex and a particular disordered bond

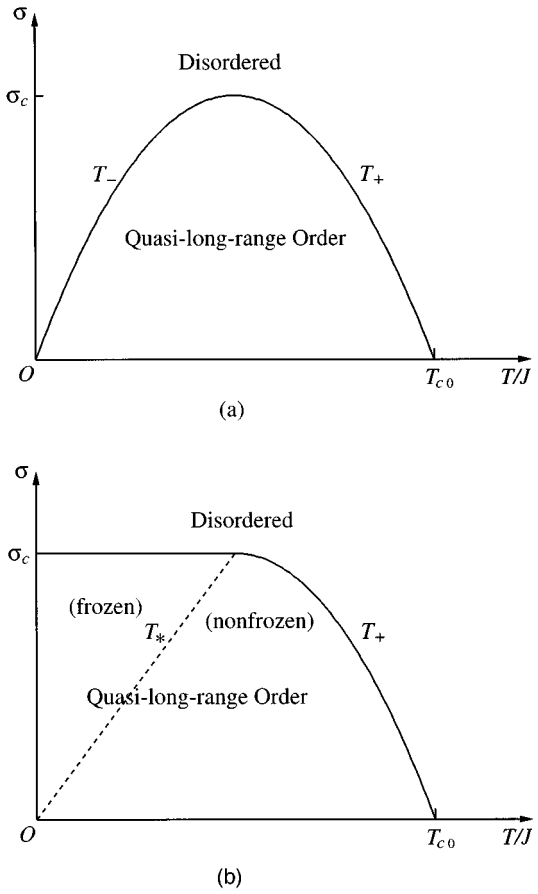

FIG. 1. Previously proposed phase diagrams of the disordered XY model. (a) Order-disorder transition at $T=T_+$ and then again at a reentrance temperature $T=T_-$. (b) No reentrance transition, but freezing of vortex-pair excitations below T_* (dashed line).

is of the charge-dipole type, with the strength of the dipole given by the phase shift A_{ij} over the bond. The equilibrium statistics of vortices is essentially decoupled from that of spin waves. Earlier renormalization-group (RG) analysis of the vortex-antivortex unbinding transition yielded a phase diagram of the kind illustrated in Fig. 1(a).[5,12] For $\sigma<\sigma_c\simeq\pi/8$, a phase with bound vortex-antivortex pairs, and hence algebraic decay of phase correlations, still exists, but only in a temperature window $T_-(\sigma)<T<T_+(\sigma)$. Below $T_-(\sigma)$, a ''reentrant'' disordered phase was predicted. The two transition temperatures coincide at a critical strength of the disorder σ_c, above which the ordered phase disappears altogether. Two recent papers, by Nattermann, Scheidl, Korshunov, and Li[18] (NSKL) and by Cha and Fertig,[19] cast doubt on the reentrance picture. The phase diagram they suggested is shown in Fig. 1(b), where the reentrance line $T_-(\sigma)$ disappears. NSKL (Refs. 18,21,22) further suggested that some sort of freezing phenomenon takes place below a certain temperature

$$T_*(\sigma)=2\sigma J \tag{1.5}$$

[see the dashed line in Fig. 1(b)], which preempts the reentrance transition at $T_-(\sigma)<T_*(\sigma)$ found previously.

The aim of the present paper is to expand the pioneering ideas presented in Refs. 18 and 19 to unfold the physics which underlies the vortex-antivortex unbinding transition in the presence of the quenched disorder. There are two main extensions contained in this work as detailed below.

First, we analyze quantitatively the equilibrium behavior of a single vortex in a background of quenched random dipoles. An analogy is made to two well-studied problems involving disorder: the random energy model[23] and a directed polymer on the Cayley tree.[24] It is shown that the single-vortex problem has a glass transition at a temperature

$$T_g=J(\pi\sigma/2)^{1/2}, \tag{1.6}$$

below which entropy goes to zero; i.e., the vortex becomes localized at the lowest-energy site. The free energy of the vortex is found to be proportional to the logarithm of system size at all temperatures. Setting the prefactor of the logarithm to zero, we obtain the phase boundary shown in Fig. 1(b).

Second, the dielectric and freezing properties of a dilute gas of vortex-antivortex pairs (or molecules) are examined in further detail, with particular emphasis on the spatial structure of equilibrium pair configurations. The freezing line $T=T_*$ in Fig. 1(b) is shown to be related to the loss of entropy of a pair over an area where the pair can be considered as isolated from other pairs of comparable size. If we fix the center position of the pair, the two vortices making up the pair freeze at T_g. In the ordered phase, $T_*<T_g$ due to the fact that the pair is allowed to explore an area much larger than its size and hence has a lower freezing temperature. Interestingly, we find that freezing of pairs is not associated with a singularity in the free energy of the system as a whole, and hence there is no real phase transition at T_*. Disorder also generates random, zero-field polarization of the gas of pairs, which enhances the effective disorder seen by vortices separated by a large distance. This effect, which has been previously overlooked, shifts the critical strength of disorder σ_c [cf. Fig. 1(b)] from $\pi/8$ to a smaller value.[22]

Results on the dilute gas of vortex-antivortex pairs are then turned into a set of RG recursion relations which capture the *average, large-distance* properties of the system. Apart from some minor differences, the RG flow equations derived in this paper are in agreement with those of Ref. 18. To the extent that such a simplifying description offers a good approximation, a phase diagram of the kind shown in Fig. 1(b) is produced.

A drawback of the RG description adopted here is that the renormalized (i.e., effective) disorder is always assumed to be Gaussian distributed, while it is clear from our analysis that the tail of the distribution dominates renormalization effects at low temperatures. This observation puts a limit on the extent the RG predictions can be trusted regarding the detailed shape of the low-temperature phase boundary, e.g., whether it contains a part which is strictly parallel to the temperature axis as in Fig. 1(b), or it could develop a positive slope to allow for reentrance of the disordered phase when σ is sufficiently close to σ_c. Qualitatively, though, there can be little doubt that the ordered phase exists down to $T=0$ when σ is far below σ_c, as the modification of the bare interactions due to excitation of large-size pairs is weak in the entire ordered phase shown in Fig. 1(b).

Another interesting question is whether the system at $\sigma>\sigma_c$ has a glassy phase at low temperatures. Our calculation of the dielectric susceptibility of a gas of pairs indicates

that screening is present at all temperatures, despite localization in the orientation of individual pairs below T_g. This supports the idea that, in the disordered phase, the vortex-vortex interaction at large distances is always short-ranged. Consequently, long-range glassy order in the phase field is not expected at any nonzero temperature due to the finite energy cost to excite an additional vortex in the system. Previous analytical and simulational studies of the gauge glass model (i.e., A_{ij} uniformly distributed in the interval $[0,2\pi]$) in two dimensions have reached the same conclusion.[20,25–27]

The paper is organized as follows. In Sec. II the Coulomb gas representation of vortices of the XY model is briefly reviewed. A qualitative discussion of vortex-antivortex unbinding is presented to highlight the outstanding issues. The problem of a single vortex interacting with quenched random dipoles is analyzed in Sec. III. A connection is made to the random energy model and to a directed polymer on the Cayley tree. In Sec. IV we examine the behavior of a dilute gas of vortex-antivortex pairs of comparable size, under the influence of disorder. The calculation of the dielectric susceptibility and the zero-field polarization of such a gas is presented, as well as an analysis of fluctuations of pair density. A physical interpretation of the T_* line is proposed. Section V contains a derivation of the RG recursion relations and results that follow from these equations. A discussion of the phase diagram, the singularity of the free energy, the divergence of the correlation length, and the two-point phase-phase correlation function is presented. The main results of the paper are summarized in Sec. VI. Some of the technical aspects of the study are relegated to the four appendixes at the end.

II. COULOMB GAS FORMULATION

A. Vortex Hamiltonian

To set the stage, let us review briefly the steps leading to the Coulomb gas representation of (1.1). The basic idea is as follows. Due to the topological nature of vortices, the XY model in two dimensions affords many metastable configurations labeled by a set of vortex charges $\{m_i\}$, where each m_i specifies the phase rotation around an elementary plaquette i, in units of 2π. The precise definition of the vortex charge configuration, derived from a given spin configuration on a lattice, requires some convention, but is otherwise unambiguous. The energy of each metastable configuration defines a vortex Hamiltonian $H_v(\{m_i\})$, while small phase fluctuations $\phi_{\mathrm{sw},i}$ around the metastable state are described by a spin-wave Hamiltonian $H_{\mathrm{sw}}(\{\phi_{\mathrm{sw}}\})$.

The simplest way to derive H_v and H_{sw} is to start from a continuum approximation of (1.1),[28,5]

$$H=\frac{J}{2}\int d^2r[\nabla\phi-a^{-1}\mathbf{A}(\mathbf{r})]^2, \tag{2.1}$$

where a is the lattice constant. The two components of $\mathbf{A}$ are given by the disorder A_{ij} on adjacent horizontal and vertical bonds, respectively.

In the presence of vortices, the field $\phi(\mathbf{r})$ is multiple valued. The vortex charges m_i fix the phase advance along a closed path surrounding site i (or rather cell i),

$$\oint d\phi=2\pi m_i.$$

In a system with periodic boundary conditions, neutrality $\Sigma_i m_i=0$ is satisfied. The gradient of the ϕ field can be decomposed into a rotation-free part and a divergence-free part,

$$\nabla\phi=\nabla\phi_{\mathrm{sw}}+\sum_i m_i\hat{\mathbf{z}}\times(\mathbf{r}-\mathbf{r}_i)/|\mathbf{r}-\mathbf{r}_i|^2, \tag{2.2}$$

where ϕ_{sw} represents ''spin-wave'' fluctuations, and $\hat{\mathbf{z}}$ is the unit vector in the third direction in space. The same procedure can be repeated for $\mathbf{A}$,

$$\mathbf{A}=a\nabla\phi_0+\mathbf{A}_{\mathrm{r}}, \tag{2.3}$$

where the potential ϕ_0 satisfies

$$a\nabla^2\phi_0=\nabla\cdot\mathbf{A}. \tag{2.4}$$

Inserting Eqs. (2.2) and (2.3) into (2.1), we obtain (apart from a constant) $H=H_{\mathrm{sw}}+H_v$, where the spin-wave part is given by

$$H_{\mathrm{sw}}=\frac{J}{2}\int d^2r(\nabla\phi_{\mathrm{sw}}-\nabla\phi_0)^2 \tag{2.5}$$

and the vortex part given by

$$H_v=\sum_i (m_i^2E_c+m_iV_i)-\pi J\sum_{i\neq j} m_im_j\ln\frac{r_{ij}}{a}. \tag{2.6}$$

(See Appendix A for more details on the derivation.) Here and elsewhere $\mathbf{r}_{ij}=\mathbf{r}_i-\mathbf{r}_j$ is the displacement vector between sites i and j, and $r_{ij}=|\mathbf{r}_{ij}|$ is the distance. In addition to the usual core energy E_c, a vortex interacts with a quenched random dipole field $\mathbf{q}_i=(a/2\pi)\mathbf{A}(\mathbf{r}_i)\times\hat{\mathbf{z}}$ through the potential

$$V_i\equiv V(\mathbf{r}_i)=2\pi J\sum_{j\neq i}\mathbf{q}_j\cdot\mathbf{r}_{ij}/r_{ij}^2. \tag{2.7}$$

From the above definition we have, in component form,

$$\langle q_{i,\alpha}\rangle=0,\quad \langle q_{i,\alpha}q_{j,\beta}\rangle=(a/2\pi)^2\sigma\delta_{ij}\delta_{\alpha\beta}. \tag{2.8}$$

Note that V_i vanishes when $\mathbf{A}$ is rotation free.

The core energy E_c can be extracted from the energy of a vortex-antivortex pair separated by a large distance.[2] Its value is nonuniversal and also depends on the choice of a.

B. Pair-unbinding transition

At sufficiently high core energies, at least, the gas of vortices in a charge-neutral system is expected to form one of the two phases described below. The first is a dielectric insulator, where ±1 charges bind to form pairs of charge-neutral molecules. This structure is low in Coulomb energy, but also low in entropy due to binding. The second is a plasma with a finite density of unpaired (or free) vortices. This structure is high in Coulomb energy but also high in entropy. In the absence of disorder, both the Coulomb energy and entropy scale logarithmically with distance in two dimensions. A simple energy-entropy argument[1] then predicts a finite-temperature transition for the unbinding of vortex-

antivortex pairs. This is also the temperature where the free energy of a single vortex goes to zero. An improved treatment, which takes into account the reduction of the Coulomb energy due to screening by other vortex-antivortex pairs, yields an exact description of the critical properties at the transition. In the plasma phase, there is complete screening of the Coulomb potential, so that interactions between distant charges become short ranged.

In the presence of quenched random dipoles, vortices may exploit fluctuations in the disorder potential to lower their Coulomb energy, and hence become more numerous. This speaks for the reduced stability of the insulating phase. On the other hand, in the process of gaining potential energy, vortices become more localized, and this way lose entropy. The first insight one needs is how much energy a vortex can gain from the disorder by positioning itself at the right place. It turns out that this problem can be solved almost exactly, and the result again has logarithmic scaling with distance. The amplitude of energy gain from disorder is proportional to $\sigma^{1/2}$ at low temperatures. Thus, when entropy is not a factor, excitation of free vortices is not expected below a certain critical strength of the disorder.

As in the pure case, a complete treatment requires analysis of the screening of the Coulomb potential due to other pairs of vortices present in the system. At high temperatures, a pair is able to explore a large number of different disorder environment, which minimizes the difference between quenched and annealed disorder. The situation becomes different at low temperatures where, as in the random energy model, the equilibrium behavior of a pair is dominated by the lowest-energy configuration in the area accessible to the pair. A crucial issue is thus to obtain the correct statistics of the pair when spatial and angular localization becomes important.

With the above general picture in mind, we are in a position to perform the necessary calculations.

III. SINGLE VORTEX

In this section, we examine the behavior of a single vortex, confined in a box of linear dimension $R \gg a$. In the presence of disorder, the energy of the vortex depends on its position i,

$$E_i = E_c + \pi J \ln(R/a) + V_i, \tag{3.1}$$

where V_i is given by (2.7) with the sum restricted to sites in the box. From the definition we have $\langle V_i \rangle = 0$. The variance and spatial correlations of V_i are given by

$$\langle V_i^2 \rangle = 2\pi\sigma J^2 \ln(R/a) + O(1), \tag{3.2}$$

$$\langle (V_i - V_j)^2 \rangle = 4\pi\sigma J^2 \ln(r_{ij}/a) + O(1). \tag{3.3}$$

A simplifying approximation to the single-vortex problem is obtained by setting the correlation of V_i to zero. The resulting problem is known as the *random energy model* (REM).[23] It turns out that, for the quantities of interest to us, correlations in the disorder potential only introduce subleading-order corrections to the REM results in the limit $R \gg a$. In the following we shall first discuss the REM and then an improved representation.

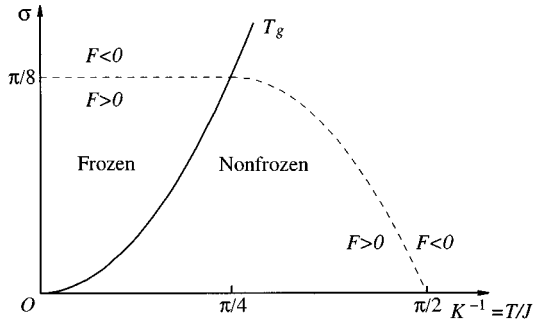

FIG. 2. Phase diagram of a single vortex. A true glass transition takes place at T_g (solid line). The free energy of the vortex vanishes along the dashed line.

A. Random energy approximation

In the REM one considers the partition function

$$z = \sum_{i=1}^{N} \exp(-x_i/T), \tag{3.4}$$

where x_i, $i = 1, \ldots, N$, are a set of random energy levels drawn independently from a Gaussian distribution,

$$\psi(x) = (2\pi\Delta)^{-1/2} \exp(-x^2/2\Delta). \tag{3.5}$$

The model has been analyzed in great detail by Derrida.[23] Below we quote some of his results relevant for our discussion, and refer the reader to his original paper for further details. (See also Appendix B.)

In the thermodynamic limit $N \to \infty$ while fixing the ratio $s \equiv \Delta/\ln N$, the average free energy is extensive in $\ln N$,

$$\langle f \rangle \equiv -T\langle \ln z \rangle = -c(T,s)\ln N + O(\ln\ln N), \tag{3.6}$$

where

$$c(T,s) = \begin{cases} T + s/(2T) & \text{for } T > T_g(s), \\ (2s)^{1/2} & \text{for } T < T_g(s). \end{cases} \tag{3.7}$$

Here

$$T_g(s) = (s/2)^{1/2} \tag{3.8}$$

is the freezing temperature of the model. For $T < T_g$, the entropy is no longer extensive in $\ln N$.

The above result can be applied to the single-vortex problem by substituting $N \to (R/a)^2$, $\Delta \to 2\pi\sigma J^2 \ln(R/a)$, and $s \to \pi\sigma J^2$. From (3.6), we obtain the average free energy of the vortex,

$$\langle F \rangle \simeq \begin{cases} E_c + \pi J \left(1 - \dfrac{2T}{\pi J} - \dfrac{\sigma J}{T} \right) \ln \dfrac{R}{a} & \text{for } T > T_g, \\ E_c + \pi J \left(1 - \sqrt{\dfrac{8\sigma}{\pi}} \right) \ln \dfrac{R}{a} & \text{for } T < T_g. \end{cases} \tag{3.9}$$

The corresponding freezing temperature is given by Eq. (1.6) (solid line in Fig. 2). The coefficient of the logarithm changes sign across the dashed line shown in Fig. 2, which is

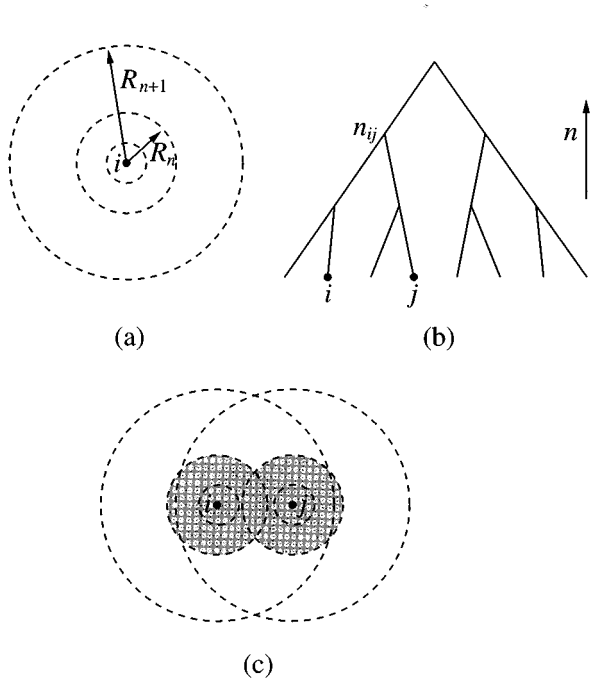

FIG. 3. Cayley tree representation of correlations in the disorder potential of a single vortex. (a) Division of the disorder potential into subsums over rings centered at vortex position i. (b) Representation of the potential by the energy of a path on the Cayley tree. The energy of a path is the sum over the energies assigned to the nodes. (c) Two sites i and j pick up nearly identical contribution from distant quenched disorder, but completely different contribution from inner shells (shadowed area) surrounding each site.

precisely the phase boundary in Fig. 1(b) when renormalized values for J and σ are used. (See discussion in Sec. V.)

Below T_g, the entropy of the vortex is no longer extensive in $\ln(R/a)$. In fact, it can be shown that only one or a few lowest-energy sites contribute significantly to the partition sum (3.4) in this regime (see Appendix B). Within the region bounded by the dashed line in Fig. 2, the typical free energy of a vortex is positive, but there are rare realizations of disorder which give rise to a negative free energy. The probability for such events is a power-law function of R/a with a negative exponent. This fact is important when we consider pair excitations in Sec. IV.

B. Correlations in the disorder potential

The REM approach to the single-vortex problem is not completely satisfactory as it ignores spatial correlations in the energies V_i. This correlation has a simple origin (see Fig. 3). When we move the vortex from a site i to a site j, the change in the disorder potential is mainly due to a change in the local environment up to a distance of order r_{ij}, as contributions to V_i and V_j from quenched dipoles farther away are nearly identical. This type of correlation can be easily coded using the Cayley tree, where each site is associated with a path on the tree. The potential on a site is made equal to the energy of a path on the tree. Geometrical proximity is translated into hierarchical proximity on the tree.

This representation can be made explicit using the following construction, though details of it should be unimportant for our conclusions. For any chosen site i, we divide the space into a set of rings of inner and outer radii R_{n-1} and R_n, respectively, such that $a=R_0<R_1<\cdots<R_m\simeq R$, while keeping $R_n/R_{n-1}=b$ constant. The potential at site i can be written as a one-dimensional sum, $V_i=\Sigma_n V_i^{(n)}$, where each term in the sum contains only contributions from dipoles within a given ring, i.e.,

$$V_i^{(n)}=2\pi J\sum_{R_{n-1}\le r_{ik}<R_n}\mathbf{q}_k\cdot\mathbf{r}_{ik}/r_{ik}^2. \tag{3.10}$$

We now identify the nth ring with the nth node (branching point) along the path i on the tree, where n increases from bottom to top. The energy of the node is given by $V_i^{(n)}$. Repeating the above procedure for a different site j, we obtain another sequence of energies $V_j^{(n)}$ for nodes on the path j. The two paths join on level $n_{ij}=\ln(r_{ij}/a)/\ln b$.

An intriguing fact about the random dipolar interaction is that the subsums constructed above are Gaussian random variables with identical statistics,

$$\langle V_i^{(n)}\rangle=0,\quad \langle V_i^{(n)}V_i^{(n')}\rangle=2\pi\sigma J^2(\ln b)\,\delta_{n,n'}. \tag{3.11}$$

Thus all rings contribute equally to the sum V_i, independent of the radius of the ring.

The Cayley tree problem discussed above has been analyzed in detail by Derrida and Spohn[24] and by Cook and Derrida.[29] Its properties are quite similar to the REM. In particular, the extensive part of the free energy is the same as in the REM, independent of the choice of b. In addition, moments of the partition function have the same dependence on N as indicated in Eq. (B11), and the transition temperature T_n of the nth moment is the same as in the REM. There are, however, differences in the amplitude of the ratio $\langle z^n\rangle/\langle z\rangle^n$. This implies that the distribution of the free energy, $f=-T\ln z$, is not exactly given by Eqs. (B8) and (B9) for f significantly less than $\langle f\rangle$, but the difference should be small, as otherwise the behavior of $\langle z^n\rangle$ would be significantly different.

C. Numerical test

The mapping to the Cayley tree problem presents a heuristic illustration of the nature of the single-vortex problem, while yields quantitative information at the same time. It is, however, difficult to estimate the error involved in the mapping. The author of this paper conjectures that the mapping is nearly exact in the sense that, when the parameters of the two problems are properly identified, the distribution of the free energy f in the two cases is related by a proportionality factor $\alpha(f)$ which is bounded, i.e., $0<\alpha_-\le\alpha(f)\le\alpha_+<\infty$, for all f and at all temperatures, in the limit $R/a\to\infty$. In the following, we report results of a numerical investigation which supports the above hypothesis.

With the choice $t=\ln(R/a)$ as the length of a path on the tree, the mapping scheme of Sec. III B yields $D=\pi\sigma J^2=2T_g^2$ and $\lambda=2$ for the parameters in Eq. (3.6) of Ref. 24. [$\lambda=2$ follows from the fact that there are $N=(R/a)^2=\exp(2t)$ sites or paths in a system of linear size R.] Equation (4.9) of Ref. 24 then predicts,

$$\frac{\langle f\rangle}{T_g}=\begin{cases} -2\left(\dfrac{T}{T_g}+\dfrac{T_g}{T}\right)\ln\dfrac{R}{a}+O(1) & \text{for } T>T_g, \\ -4\ln\dfrac{R}{a}+\dfrac{1}{2}\ln\ln\dfrac{R}{a}+O(1) & \text{for } T=T_g, \\ -4\ln\dfrac{R}{a}+\dfrac{3}{2}\ln\ln\dfrac{R}{a}+O(1) & \text{for } T<T_g. \end{cases} \tag{3.12}$$

(Note that there is a crossover in the behavior of the subleading-order term when T is close to T_g, which we shall not elaborate here.) It is expected that, up to terms of order unity, the above expressions are insensitive to the assumption that the random energies are Gaussian distributed, and hence have a certain degree of universality.[29] The REM model, on the other hand, predicts a prefactor $\frac{1}{2}$ for the subleading-order term in (3.12) in the entire low-temperature phase.

Our numerical task is to check the validity of (3.12) up to the subleading-order term by varying R and T. The first step of the exercise involves generation of the random potentials V_i. In principle, this can be done by assigning random dipole moments with a fixed variance to each site on a $(R/a)\times(R/a)$ lattice, and then carry out the sum (2.7) for each site i on the dual lattice where the vortex is supposed to sit. An appropriate choice of the boundary condition is that, in computing the displacement vector $\mathbf{r}_{ij}$ in (2.7) between sites i and j, we consider all periodic continuations of j, and choose the one which is closest to i. Alternatively, we can generate V_i directly with the desired statistical properties by noting that their variance and correlations as expressed by Eqs. (3.2) and (3.3) are identical to those of a Gaussian surface in two dimensions.[30] Since the Fourier components of such a surface fluctuate independently, they can be obtained directly with the prescribed variance using a Gaussian random number generator. A fast Fourier transform algorithm can then be used to obtain V_i. This method, which is far more efficient than the former, is used in our Monte Carlo calculation of the disorder-averaged free energy.

We have investigated systems of linear size $R/a=4,8,\ldots,512$. The free energy is evaluated at five different temperatures for each disorder realization, and then averaged over 20 000 independent realizations. The statistical error in $\langle f\rangle/T_g$ so obtained is less than 0.025. Figure 4 shows the data on a semilogarithmic scale. To achieve a closer comparison with the analytical prediction, the expected low-temperature leading-order term has been taken away from the data. For $T=0$ and $T=0.5T_g$, the subleading-order correction can be well fitted to the form $\frac{3}{2}\ln[2+\ln(R/a)]+\text{const}$ (solid line), while at $T=T_g$, the form $\frac{1}{2}\ln[2+\ln(R/a)]+\text{const}$ (dashed line) fits better. For $T=1.5T_g$ and $2T_g$, a residual logarithmic term is clearly seen, indicating that the system is no longer in the frozen phase. The slopes of these two sets of data agree well with the predicted values $-\frac{1}{3}$ and -1, respectively.

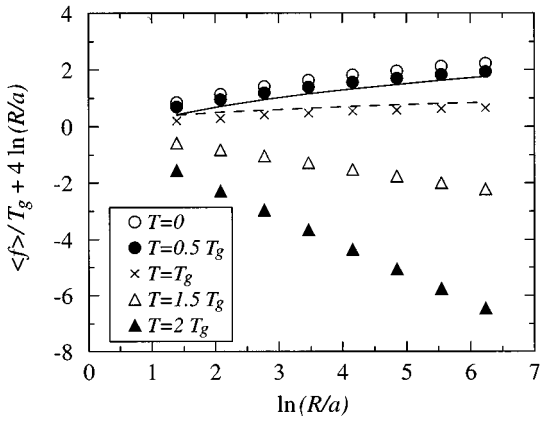

FIG. 4. The average free energy (scaled by the glass transition temperature T_g) of a single vortex in a box of linear size R/a, with the expected $T=0$ leading-order behavior subtracted out. Solid and dashed lines are fits to the predicted subleading-order behavior for $T<T_g$ and $T=T_g$, respectively.

IV. DILUTE GAS OF PAIRED VORTICES

As mentioned in Sec. II B, a quantitative study of the pair-unbinding transition must include a discussion of pair excitations which modify the Coulomb interaction at large distances. This is usually done by employing a real-space RG procedure, to be explained in detail in Sec. V. A crucial step in the RG scheme is the calculation of the dielectric susceptibility and zero-field polarization of a gas of pairs in a certain size range, say, between R and $R+dR$. This is the task to be carried out in this section.

A. Lattice-gas representation

To treat a dilute gas of pairs of uniform size R, it is conceptually helpful to separate the ''internal'' degrees of freedom of a pair, given by allowed configurations of the pair confined to a box of linear size R, from rigid translations of the pair over a distance greater than R. One way of implementing the idea is to impose a lattice with a lattice constant R. The lattice-gas representation is extremely useful owing to the following two properties of the system: (i) The disorder potential on a pair is essentially uncorrelated when the pair is translated over a distance larger than R; (ii) interaction between pairs of similar size in the dilute limit can be approximated by a hard-core potential extending over a distance of the pair size R. These facts can be established following a similar line of reasoning as in the original paper by Kosterlitz and Thouless.[1]

Let $\mathbf{r}^+$ and $\mathbf{r}^-$ be the coordinates of $+1$ and -1 charges in a pair, respectively. The pair energy is given by

$$E_p=2E_c+2\pi J\ln(R/a)+V(\mathbf{r}^+)-V(\mathbf{r}^-), \tag{4.1}$$

where $R=|\mathbf{r}^+-\mathbf{r}^-|$ is the size of the pair.

The rapid decay of correlations in the disorder potential $V(\mathbf{r}^+)-V(\mathbf{r}^-)$ of a pair beyond a distance of order R comes from an observation made in Sec. III B. The two charges which make up a pair interact separately with quenched random dipoles within a distance of order R from the pair center, but collectively as a dipole when more distant disorder is

in question. Hence the random part of E_p is dominated by disorder within a distance of order R from the pair center. (The remaining contribution from distant quenched random dipoles can be treated as a perturbation when necessary.) On the other hand, barring contributions from distant quenched dipoles, $V(\mathbf{r}^+)$ is quite independent from $-V(\mathbf{r}^-)$ for two reasons. First, each potential is dominated by quenched dipoles in the immediate vicinity of the site in question (see discussion on the ring structure in Sec. III B). Second, although the two charges are in the same disorder environment, when it comes to optimizing their (free) energies, they see opposite ends of the disorder energy distribution due to the difference in sign. Therefore, to a good approximation, we can replace E_p by the sum of two single-vortex energies of the form (3.1), each containing a random potential generated by quenched dipoles within a box of linear size R, independent from the other.

The interaction between one pair and another is of the dipole-dipole form at large distances, which is small compared to E_p and can be treated as a perturbation. The interaction becomes more complex when two pairs are at a distance $R_1<R$, but it is generally repulsive, with a strength of order $4\pi J\ln(R/R_1)$. (Note that the two pairs should be arranged in such a way that it is not possible to regroup them to form ± 1 pairs of smaller sizes.) For simplicity, we shall replace the interaction by a hard-core potential of range R. In the dilute limit, the main effect of this interaction is to prevent more than one pair from taking advantage of a particular favorable configuration (and the ones very close to it), which turns out to be a very important constraint at low temperatures.[18]

We are now in a position to define the lattice-gas representation. We divide the plane into a square lattice of cells, each of linear dimension R. Any given cell has at most one pair, and pairs in different cells do not interact with each other. The Boltzmann weight on an occupied cell can be written as $y_p z_p$, where

$$y_p \equiv (R/a)^{-2\pi J/T}\exp(-2E_c/T) \tag{4.2}$$

is the *pair fugacity* and z_p is the configurational partition function of the pair attached to the cell. Since there is no interaction between different cells, the partition function of the system factorizes into a product of cell partition functions $1+y_p z_p$. In addition, the average over all cells can be replaced by an average over the disorder, as each cell represents an independent realization.

To apply the lattice-gas description to the system of pairs in a given size range, say, between R and $R+dR$, we need to specify z_p in more detail. For the discussion to be meaningful, dR should be small enough so that the pair fugacity y_p can be regarded as a constant, but large enough so that individual charges in a pair are allowed to explore their own local disorder environment without been severely constrained by the specified range of pair size. Both criteria can be met by choosing $dR\sim R$. The configurational partition function of an occupied cell is given by

$$z_p = \sum_{\substack{(\mathbf{r}^+ + \mathbf{r}^-)/2 \in \text{cell} \\ R \le |\mathbf{r}^+ - \mathbf{r}^-| < R+dR}} \exp\left[-\frac{V(\mathbf{r}^+)-V(\mathbf{r}^-)}{T}\right]. \tag{4.3}$$

The potential $V(\mathbf{r}^+)-V(\mathbf{r}^-)$ inside a cell has a spatial correlation of similar nature as the potential on a single vortex discussed in Sec. III. To simplify the calculation, we shall again make the random energy approximation where this correlation is ignored. The parameters of the REM applied to the problem of pairs are

$$N = 2\pi(R/a)^4(dR/R), \quad \Delta = 4\pi\sigma J^2\ln(R/a). \tag{4.4}$$

For $dR\simeq R$, the freezing temperature T_g for the pair in a cell is the same as the freezing temperature of a single vortex, Eq. (1.6).

B. Pair density

In equilibrium, the probability of finding a pair in a given cell is given by

$$W = \frac{y_p z_p}{1+y_p z_p}. \tag{4.5}$$

For a dilute gas, the typical value of W is given by $W_{\text{typ}}\simeq y_p z_{p,\text{typ}}$, where $z_{p,\text{typ}}$ is the typical value of z_p (see discussion in Appendix B). Combining Eqs. (3.6), (3.7), (B6), and (4.2), we obtain,

$$W_{\text{typ}} \sim \begin{cases} \left(\dfrac{R}{a}\right)^{4-2\pi K+2\pi\sigma K^2}\dfrac{dR}{R} & \text{for } T>T_g, \\ \left(\dfrac{R}{a}\right)^{-2\pi K(1-\sqrt{8\sigma/\pi})}\dfrac{dR}{R} & \text{for } T<T_g. \end{cases} \tag{4.6}$$

Here $K\equiv J/T$. The exponent of the power law changes sign across the dashed line in Fig. 2.

Like z_p, W has a broad distribution. Its mean value $\langle W\rangle$ deviates significantly from W_{typ} for $T<T_g$. Since the nth moment of z_p grows much faster than $\langle z_p\rangle^n$ for sufficiently large n, it is not possible to calculate $\langle W\rangle$ by expanding the right-hand side of (4.5) as a power series of $y_p z_p$. Nevertheless, the average can be calculated by treating the cases $y_p z_p<1$ and $y_p z_p>1$ separately, as done in Appendix C. Results of the calculation are given by Eqs. (C11) and (C13) in respective temperature regimes. For $R\gg a$, a power-law dependence of $\langle W\rangle$ on R is found,

$$\langle W\rangle \sim \begin{cases} \left(\dfrac{R}{a}\right)^{4-2\pi K+2\pi\sigma K^2}\dfrac{dR}{R} & \text{for } T>T_*, \\ \left(\dfrac{R}{a}\right)^{4-\pi/(2\sigma)}\dfrac{dR}{R} & \text{for } T<T_*. \end{cases} \tag{4.7}$$

The exponent freezes to a temperature-independent value below $T_*=2\sigma J$.

C. Zero-field polarization

The disorder environment in a given cell specifies a favorable configuration for a pair in the cell. The breaking of rotational invariance thus yields a zero-field dipole moment

$$\mathbf{p}_0 \equiv \frac{\Sigma \mathbf{p}\exp[-E_p/T]}{1+y_p z_p}, \tag{4.8}$$

where $\mathbf{p}=\mathbf{r}^{+}-\mathbf{r}^{-}$. The sum in Eq. (4.8) is restricted to the internal degrees of freedom of the pair, as in Eq. (4.3).

Due to statistical rotational symmetry, $\langle \mathbf{p}_0 \rangle = 0$. Its variance can be calculated approximately from the following consideration. Note that $\mathbf{p}_0$ is small when many distinct configurations contribute to the cell partition sum z_p. It becomes large when the lowest-energy configuration (and nearby configurations with approximately the same orientation of $\mathbf{p}$) dominates. Based on the discussion of Appendix B, it is reasonable to assume that the latter occurs whenever z_p is significantly larger than its typical value, $z_{p,\mathrm{typ}}$. Replacing $\mathbf{p}$ inside the sum in (4.8) by the dipole moment of the ground state, we make an error with a probability of the order of W_{typ}, which is smaller than $\langle W \rangle$. This yields the estimate

$$\langle |\mathbf{p}_0|^2 \rangle / R^2 = \langle W^2 \rangle + O(\langle W \rangle^2). \tag{4.9}$$

The calculation presented at the end of Appendix C yields, for $T < T_*$,

$$\langle W^2 \rangle \simeq (1 - T/T_*) \langle W \rangle. \tag{4.10}$$

For $T > T_*$, $\langle W^2 \rangle$ decays faster with R than $\langle W \rangle$. The distribution of $|\mathbf{p}_0|$ is expected to be broad. In particular, for $T < T_g$, where typically one or two configurations dominate the partition sum, the distribution of $|\mathbf{p}_0|$ is similar to the distribution of W.

Let us now consider the correlation between $\mathbf{p}_0$ and the total dipole moment of disorder in the cell,

$$\mathbf{q} = \sum_{i \in \mathrm{cell}} \mathbf{q}_i . \tag{4.11}$$

Since $\mathbf{p}_0$ is mostly determined by the arrangement of the disorder in the immediate vicinity of the two charges making up the pair, we expect the contribution to $\mathbf{p}_0$ from $\mathbf{q}$ to be small, but the effect is important for later discussions. To estimate the contribution, let us consider a quantity $\tilde{\mathbf{p}}_0$, which is the equivalent of $\mathbf{p}_0$ under the replacement $\mathbf{q}_i \to \tilde{\mathbf{q}}_i = \mathbf{q}_i - (a/R)^2 \mathbf{q}$. From the third example of Appendix A, we see that switching on $\mathbf{q}$ is equivalent to switching on a polarizing field $\mathbf{E}_q = -2\pi^2 J \mathbf{q}/R^2$. Linear response theory then suggests, on average, a relation of the form

$$\mathbf{p}_0 \simeq \tilde{\mathbf{p}}_0 - 2\pi^2 \overline{\chi} J \mathbf{q}, \tag{4.12}$$

where $\overline{\chi}$ is the average dielectric susceptibility of the gas of pairs, to be discussed below.

D. Induced polarization

In the presence of a weak, constant external electric field $\mathbf{E}$, a cell acquires an induced dipole moment due to pair excitation,

$$\mathbf{p}_{\mathrm{ind}} = \frac{\Sigma \mathbf{p} \exp[-(E_p - \mathbf{p}\cdot\mathbf{E})/T]}{1 + \Sigma \exp[-(E_p - \mathbf{p}\cdot\mathbf{E})/T]} - \mathbf{p}_0 . \tag{4.13}$$

The induced polarization $\mathbf{P}_{\mathrm{ind}}$ of the gas of pairs is given by the spatial average of $\mathbf{p}_{\mathrm{ind}}$ or, equivalently, the disorder average,

$$\mathbf{P}_{\mathrm{ind}} = R^{-2} \langle \mathbf{p}_{\mathrm{ind}} \rangle. \tag{4.14}$$

To the first order in $\mathbf{E}$, we find

$$\mathbf{P}_{\mathrm{ind}} = \overline{\chi} \mathbf{E}, \tag{4.15}$$

where

$$\overline{\chi} = (2T)^{-1} (\langle W \rangle - \langle |\mathbf{p}_0|^2 \rangle / R^2). \tag{4.16}$$

Using Eqs. (4.5) and (4.9) we may rewrite the above equation as

$$\overline{\chi} = \frac{1}{2T} \left[y_p \frac{\partial \langle W \rangle}{\partial y_p} + O(\langle W \rangle^2) \right]. \tag{4.17}$$

Here we have used the identity

$$y_p \partial \langle W \rangle / \partial y_p = \langle W \rangle - \langle W^2 \rangle. \tag{4.18}$$

The derivative in the above equation can be evaluated using Eq. (C10) for $T > T_*$ and (C12) for $T < T_*$. To leading order, the result reads

$$\overline{\chi} \simeq \begin{cases} (2T)^{-1} \langle W \rangle & \text{for } T > T_*, \\ (2T_*)^{-1} \langle W \rangle & \text{for } T < T_*. \end{cases} \tag{4.19}$$

[Note that, in both cases, the coefficient in front of $\langle W \rangle$ is fixed by the (effective) power-law dependence of $\langle W \rangle$ on y_p. Hence (4.19) is more exact than what one might have expected from the approximate nature of Eqs. (C10) and (C12).]

The dielectric susceptibility is finite down to $T = 0$. At $T = 0$, individual pairs cannot respond to a weak applied field due to loss of entropy. The polarizability of the medium is a consequence of a finite density of states at zero pair energy. Pair configurations with a slightly positive energy in the absence of the field may acquire a negative energy if it is favored by the field, and hence become occupied. The opposite happens for the unfavored pair configurations opposing the field direction.

E. Pair-freezing temperature T_*

The change in the leading order behavior of the pair density $\rho \sim \langle W \rangle / R^2$ at T_* [Eq. (4.7)] has a simple interpretation. Given the strong repulsive interaction between two pairs at a distance smaller than their size R, and the absence of correlation in the disorder potential on a pair beyond a distance of order R, it is reasonable to assume that clustering of pairs is rare in the dilute limit. The typical distance between neighboring pairs is thus given by $L = \rho^{-1/2} > R$. Within an area of linear size L, we have typically one pair only.

Let us first consider the equilibrium statistics of a single pair in a box of linear size L, taken to be arbitrary for the moment. The total number of configurations available to the pair is $N = (R/a)^2 (L/a)^2$, and the variance of the random potential, $\Delta = 4\pi\sigma J^2 \ln(R/a)$. In the random energy approximation, the mean free energy of the pair follows from Eq. (3.6),

$$F_p(L,T) \simeq 2E_c + 2\pi J \ln(R/a) - 2c(T,s)[\ln(R/a) + \ln(L/a)], \tag{4.20}$$

where

$$s=\frac{2\pi\sigma J^2\ln(R/a)}{\ln(R/a)+\ln(L/a)}. \tag{4.21}$$

For a fixed L, $F_p(L,T)$ increases with decreasing T, and locks to a constant for $T<T_g(s)$. At a fixed temperature, $F_p(L,T)$ decreases with increasing L.

The typical interpair distance $L(T)$ is determined by the condition

$$F_p(L,T)=0. \tag{4.22}$$

From the properties of F_p mentioned above, we see that $L(T)$ increases as T decreases, and locks to a constant L_* for $T<T_*$. Here $T_*=T_g(s_*)$ is obtained self-consistently, with s_* given by (4.21) at $L=L_*$. The result for T_* agrees with (1.5). For $T>T_*$, we may use the high-temperature expression for $c(T,s)$ in (4.20), and the condition (4.22) yields the following estimate for the number of pairs in an area of size R:

$$(R/L)^2\simeq(R/a)^{4-2\pi K+2\pi\sigma K^2}\exp(-2E_c/T), \tag{4.23}$$

in agreement with (C11). The length L_* satisfies

$$(R/L_*)^2\simeq(R/a)^4\exp(-\Delta/2T_*^2), \tag{4.24}$$

in rough agreement with (C12) for the number of pairs in an area of size R below T_*.

The physical meaning of the temperature T_* is now clear. For $T>T_*$, the entropy of a pair in a region of the size of interpair distance is finite and varies smoothly with T. This entropy is lost at T_*. Therefore T_* is associated with the pair freezing. The length scale $L_*(R)$ is the smallest size of an area where one typically finds a negative ground-state energy for a pair of size R.

In contrast, the single-vortex glass temperature T_g is associated with the loss of entropy for a pair when it is restricted to an area of pair size. [Note that (4.21) reduces to the expression for a single vortex when we set $L=R$.] This temperature does not play a special role in the *equilibrium* behavior of a pair, where the relevant length scale is set by the interpair distance. Likewise, as far as the equilibrium properties of a dilute gas of pairs are concerned, the cell representation we employed is merely a convenient device for performing calculations.

The equivalence of our results to those of Refs. 18 and 22 implies that there is a simple connection between the two approaches. In the work of NSKL and the more recent paper by Scheidl, calculation of thermal averages were made under the ''factorization ansatz,'' which assumes that pairs do not interact unless they take identical positions. From the discussion of Sec. IV A we see that the pair-pair repulsion extends to a distance of the order of pair size R. If there is no strong reason provided by disorder for clustering of pairs, the two approaches should differ only by a relative amount proportional to the pair density; i.e., the difference should show up only at order $\langle W\rangle^2$ in the expressions for $\overline{\chi}$, etc. This is precisely what happens under the random-energy approximation. In reality, due to correlations in the disorder potential, close to a very favorable configuration for a pair, there are other configurations which are nearly as favorable, though pair-pair repulsion would forbid simultaneous occupation of these configurations. The true density of pairs is thus expected to be somewhat smaller than the one calculated under the factorization ansatz or the random energy approximation. Nevertheless, from what we understand about the correlations, the qualitative behavior of the system should be the same as predicted by the approximate calculations. In particular, no change in the exponent of the power laws in Eq. (4.7) is expected.

V. RECURSION RELATIONS AND RESULTS

A. RG transformation

The knowledge we gained about a dilute gas of vortex-antivortex pairs can now be incorporated into a RG procedure aimed at capturing the large-distance behavior of the Coulomb gas with disorder. This can be done explicitly following an integration scheme used previously by Kosterlitz for treating the pure problem.[2]

Consider a configuration $\{m_i\}$ made up of two groups of charges. The first group, $\{m_i^<\}$, consists of pairs of ±1 vortices, each of size less than a cutoff size R. The second group, $\{m_i^>\}$, consists of charges which do not fall into that category. (Note that our usage of the superscripts ''$<$'' and ''$>$'' is the opposite of the one familiar in a momentum-space RG.) The total energy of the system, Eq. (2.6), can be rewritten as

$$H_v(\{m_i\})=H_v(\{m_i^<\})+H_v(\{m_i^>\})+H_{\rm int}(\{m_i^<\},\{m_i^>\}), \tag{5.1}$$

where

$$H_{\rm int}\simeq-\sum_n \mathbf{p}_n\cdot\mathbf{E}^>(\mathbf{r}_n) \tag{5.2}$$

describes the interaction between the two groups. Here $\mathbf{p}_n$ is the dipole moment of pair n in the first group, $\mathbf{r}_n$ is the center position of the pair, and

$$\mathbf{E}^>(\mathbf{r})=2\pi J\sum_i m_i^>\frac{\mathbf{r}-\mathbf{r}_i}{|\mathbf{r}-\mathbf{r}_i|^2} \tag{5.3}$$

is the electric field at $\mathbf{r}$ due to the presently unpaired charges in the second group.

The partition sum over the paired charges is given by

$$\Xi^<=\sum_{\{m_i^<\}}\exp(-[H_v(\{m_i^<\})+H_{\rm int}]/T). \tag{5.4}$$

Writing $\Xi^<\equiv\Xi_0^<\exp(-\delta H/T)$, where $\Xi_0^<$ is the partition function at $H_{\rm int}=0$, we obtain

$$\delta H(\{m_i^>\})=-T\ln\langle\exp(-H_{\rm int}/T)\rangle_0, \tag{5.5}$$

where $\langle\cdots\rangle_0$ denotes thermal average with respect to $H_v(\{m_i^<\})$. Treating $H_{\rm int}$ as a perturbation, we can write δH in a more suggestive form

$$\delta H=-\int d^2r[\mathbf{P}_0(\mathbf{r})+\tfrac{1}{2}\mathbf{P}_{\rm ind}(\mathbf{r})]\cdot\mathbf{E}^>(\mathbf{r})+O(|\mathbf{E}^>|^3). \tag{5.6}$$

Here $\mathbf{P}_0(\mathbf{r})=\langle\Sigma_n\mathbf{p}_n\delta(\mathbf{r}-\mathbf{r}_n)\rangle_0$ is the zero-field polarization of the paired charges in the absence of the interaction term

$H_{\rm int}$, and $\mathbf{P}_{\rm ind}=\mathbf{P}-\mathbf{P}_0$ is the induced polarization of the paired charges due to the field $\mathbf{E}^>$. [Note that $\mathbf{P}(\mathbf{r})$ is defined in the same way as $\mathbf{P}_0(\mathbf{r})$ except that the thermal averaging is taken with respect to $H_v(\{m_i^<\})+H_{\rm int}$.]

The renormalization-group idea is to take the cutoff size R as a running parameter, and perform the elimination of paired charges $\{m_i^<\}$ in a step-by-step manner, so that each time one needs to deal with pairs in a narrow size range R to $R+dR$ only. The necessary calculations have already been done in Sec. IV. Substituting Eq. (4.15) into (5.6), we obtain

$$\delta H \simeq -\int d^2r[\mathbf{P}_0\cdot\mathbf{E}^> + \tfrac{1}{2}\overline{\chi}|\mathbf{E}^>|^2]. \tag{5.7}$$

This is nothing but the field integral version of the Coulomb energy (2.6), and hence can be incorporated into $H_v(\{m_i^>\})$ by redefining the parameters J and σ of the model.

The change in J can be obtained with the help of the first example in Appendix A. One thing to note is that the integral over $|\mathbf{E}^>|^2$ in (5.7) excludes regions of size R around each $m_i^>$ charge, since paired vortices should not be found in these areas. This leads to the identification $b=R$ in Eq. (A8). The new effective parameters are given by

$$E_c \rightarrow \widetilde{E}_c = E_c + 4\pi^3\overline{\chi}J\ln(R/a) \tag{5.8}$$

and

$$J\rightarrow \widetilde{J}^{-1} = J^{-1} + 4\pi^2\overline{\chi}, \tag{5.9}$$

equivalent to Eq. (A4).[31] The extra term in $\widetilde{E}_c$ merely accounts for the fact that screening from this group of pairs is effective only at distances larger than R.

In Sec. IV C, contribution to the zero-field dipole moment $\mathbf{p}_0$ of a cell due to disorder within the cell was calculated. More distant disorder contributes to $\mathbf{p}_0$ by acting as an additional polarizing field. When the latter contribution is substituted into Eq. (5.7), we see that, with the help of the second example in Appendix A, the interaction strength between $\{m_i^>\}$ and quenched dipoles $\mathbf{q}_j$ is reduced by a factor $1-2\pi^2\overline{\chi}J$. Combining the zero-field polarization $\mathbf{P}_0=\mathbf{p}_0/R^2$ of pairs with the disorder polarization $\mathbf{Q}=\mathbf{q}/R^2$, we obtain the effective disorder that couples linearly to $\mathbf{E}^>$ in the Hamiltonian $H_v+\delta H$ for the $\{m_i^>\}$ charges,

$$\mathbf{Q}_{\rm eff}=(1-4\pi^2\overline{\chi}J)\mathbf{Q}+\widetilde{\mathbf{P}}_0, \tag{5.10}$$

where $\widetilde{\mathbf{P}}_0=\widetilde{\mathbf{p}}_0/R^2$ is independent of $\mathbf{Q}$ [see discussion around Eq. (4.12)].

Equation (5.10) shows that pair excitations modify the quenched disorder seen by $\{m_i^>\}$ charges in two distinct ways. The first effect is the screening of the interaction at distances larger than the pair size R, which can be taken into account by a redefinition of J, Eq. (5.9). The second effect is the generation of additional disorder. Since $\widetilde{\mathbf{P}}_0$ is independent of $\mathbf{Q}$, we obtain an additive contribution to the variance of disorder, σ. Writing $\widetilde{J}\widetilde{\mathbf{Q}}=J\mathbf{Q}_{\rm eff}$, and using $\langle|\mathbf{Q}|^2\rangle\equiv\sigma/(2\pi^2R^2)$, we get

$$\widetilde{\sigma}=\sigma+2\pi^2\langle W^2\rangle+O(\langle W\rangle^2). \tag{5.11}$$

In deriving the above expression we used the fact that the difference between the variance of $\mathbf{P}_0$ and that of $\widetilde{\mathbf{P}}_0$ is of order $\langle W\rangle^2$. Using the result for $\langle W^2\rangle$, we see that the change in σ is proportional to $\langle W\rangle$ for $T<T_*$, but of higher order for $T>T_*$.

Equations (5.9) and (5.11) can be expressed in the usual differential form by writing $R=ae^l$. For convenience, we introduce a dimensionless quantity $Y(R)$, such that $2\pi Y^2 dR/R\equiv\langle W\rangle$ gives the number of vortex-antivortex pairs of size between R and $R+dR$, in an area of size R^2 and averaged over the whole system. For $T>T_*$ or $K^{-1}\equiv T/J>K_*^{-1}=2\sigma$, we have

$$dK^{-1}/dl = 4\pi^3Y^2, \tag{5.12a}$$

$$d\sigma/dl = 0, \tag{5.12b}$$

$$dY/dl = (2-\pi K+\pi\sigma K^2)Y. \tag{5.12c}$$

For $T<T_*$ or $K^{-1}<K_*^{-1}$, we have

$$dK^{-1}/dl = 2\pi^3\sigma^{-1}K^{-1}Y^2, \tag{5.13a}$$

$$d\sigma/dl = 2\pi^3(2-\sigma^{-1}K^{-1})Y^2, \tag{5.13b}$$

$$dY/dl = \left(2-\frac{\pi}{4\sigma}\right)Y. \tag{5.13c}$$

Note that, in writing the above equations, we only kept terms up to order Y^2. The flow equations for Y follow from the power-law dependence of the pair density on pair size as given by Eqs. (C11) and (C13). A term of order $1/l$ inside the brackets in (5.13c) has been neglected.

A few remarks concerning the above recursion relations are in order. For $T>T_*$, Eqs. (5.12) are identical to those of previous authors.[5,12] From Eq. (5.11) we see that there is a renormalization of σ even in this regime, but the effect is of higher order than Y^2. The change of the flow equations for $T<T_*$ was pointed out earlier by NSKL.[18] The renormalization of σ, though not recorded previously, has also been obtained by Scheidl using a different approach.[22]

In the absence of disorder, Y is equal to the ''rescaled'' single vortex fugacity, $(R/a)^{2-\pi J/T}\exp(-E_c/T)$, in the dilute limit. When disorder is present, the relation between Y and the core energy E_c is more complicated. The bare value of Y can be obtained from Eqs. (C11) and (C13) for $T>T_*$ and $T<T_*$, respectively. It has a finite limit Y_0 at $T=0$. For small σ, $Y_0^2\sim\sigma^{1/2}\exp(-c/\sigma)$, where c is a positive, model-dependent number. At small values of T, the bare value of Y increases from Y_0 by an amount proportional to T^2.

B. Phase diagram and thermodynamic properties

1. Constants of RG flow

Seemingly complex at first sight, the flow equations (5.12) and (5.13) have in fact the same structure as their $\sigma=0$ counterpart.[2] The fixed points of the flow are located on the $Y=0$ plane in the three-dimensional (3D) parameter space spanned by K^{-1}, σ, and Y. They are stable in the region enclosed by the dashed line in Fig. 5, but unstable outside the region. Points on the dashed line are hyperbolic fixed points which describe the pair-unbinding transition.

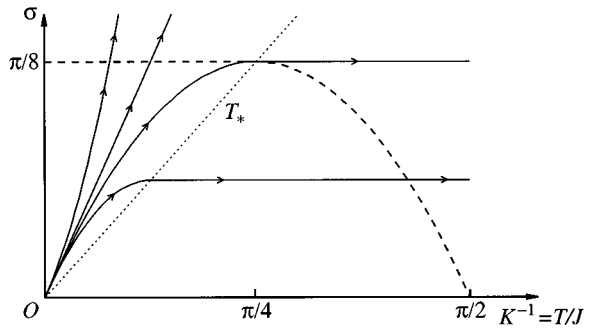

FIG. 5. Renormalization-group flows on the σ-K^{-1} plane. Solid lines are trajectories of the RG flow, with arrows indicating the flow direction. The flow follows a parabola up to T_* (dotted line), and is then joined smoothly by a horizontal line at $T>T_*$. The dashed line is the line of hyperbolic fixed points of the RG flow, which gives the phase boundary at $Y=0$.

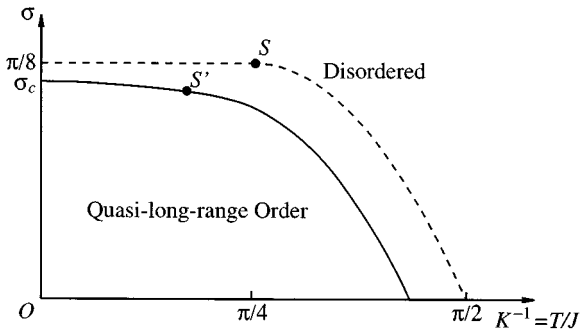

FIG. 6. Schematic phase diagram from present work. Solid line indicates the order-disorder phase boundary in terms of bare parameters of the model. It lies inside the region enclosed by the dashed line, which is the line of the phase transition when renormalized values are plotted. At the special point S and its counterpart S', where the T_* line meets the phase boundary, a slightly different critical behavior is expected. See the text.

It turns out that the flow equations are completely integrable. In the region $T>T_*$ [to the right of the dotted line in Fig. 5],

$$\sigma=\text{const} \tag{5.14a}$$

is obviously a constant of the flow. On the $T<T_*$ side, the corresponding first integral is given by

$$K-\sigma K^2=\text{const}, \tag{5.14b}$$

as can be easily verified using Eqs. (5.13a) and (5.13b). These ''streamlines'' of the flow are illustrated in Fig. 5.

The second constant of the flow is given by

$$Y^2-\pi^{-3}\left(K^{-1}-\frac{\pi}{2}\sigma K+\frac{\pi}{2}\ln K\right)=\text{const} \tag{5.15a}$$

for $T>T_*$, and

$$Y^2-\pi^{-3}\left(K^{-1}+\sigma+\frac{\pi}{4}\ln K\right)=\text{const} \tag{5.15b}$$

for $T<T_*$. A unique trajectory in the 3D parameter space is specified when one combines (5.15) with (5.14), with the constants fixed by bare values of the parameters involved.

2. Phase diagram

The original XY model has only two parameters $K_B^{-1}=T/J$ and σ_B. The bare value of Y, Y_B, is a function of K_B and σ_B. The phase boundary of the model is determined by the condition that the RG flow ends on the dashed line in Fig. 5. Since the flow takes both σ and K^{-1} to larger values, this phase boundary lies within the area bounded by the dashed line, as illustrated in Fig. 6.

The question of the reentrance of the disordered phase is whether the upper-left part of the phase boundary illustrated in Fig. 6 contains a piece with a positive slope. Although earlier calculations which led to the prediction of a reentrance transition are not to be trusted, it is actually difficult to rule out such a possibility from the new RG flow equations (5.13). From Eq. (5.13b) we see that, at a given Y^2, the increase in the effective disorder becomes slower as temperature increases. Hence, for a fixed Y_B, the bare value of σ which flows to the fixed point value $\sigma=\pi/8$ increases with increasing T/J. On the other hand, in the original XY model, the bare pair density Y_B^2 at a fixed σ is expected to increase with temperature, too. The calculation presented in this paper is not quantitative enough to assess the two competing effects to reach a precise conclusion on the shape of the low-temperature part of the phase boundary.

3. Approach to criticality

The critical behavior around the transition is controlled by the RG flow close to the relevant hyperbolic fixed point. As an example, let us consider flows along a particular contour in Fig. 5. Substituting Eqs. (5.14) into Eqs. (5.15), we get a flow pattern depicted in Fig. 7. The curve consists of two pieces, one from Eqs. (5.14b) and (5.15b) for $K^{-1}<K_*^{-1}$, and the other from Eqs. (5.14a) and (5.15a) for

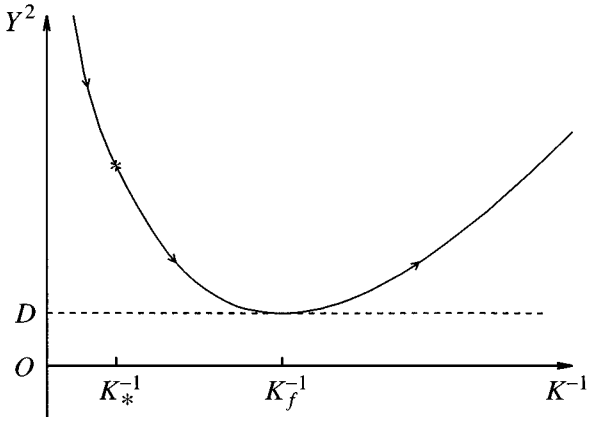

FIG. 7. The RG flow trajectory on the Y^2-K^{-1} plane. (This example corresponds to the lowest of the four flow lines illustrated in Fig. 5.) At the transition, the bottom of the curve touches the horizontal axis ($D=0$). Generically, the curve is quadratic around the minimum at $K^{-1}=K_f^{-1}$. However, for $K_f^{-1}=K_*^{-1}$, a cubic singularity is found instead.

$K^{-1}>K_*^{-1}$. Since Eqs. (5.14) do not involve Y^2, any vertical translation of the curve shown in Fig. 7 is also an invariant of the RG flow. This family of curves can be parametrized by the minimum value of Y^2 on each curve, D.

In the ordered phase and at the transition, the scaled pair density Y^2 eventually reaches zero on large length scales. The corresponding RG flow follows a curve with $D\leqslant 0$, with the marginal case $D=0$ reserved for the transition. On the disordered side but close to the transition, the RG flow follows a curve with a small positive D. Along such a curve, the value of Y^2 first decreases as the running parameter l increases, becomes almost stationary around the minimum of the curve, and then grows rapidly to large values beyond $l=l_+$. The length $\xi_+=a\exp(l_+)$ sets the scale where the correlation function (see Sec. V C below) turns from a power law to an exponential decay.

The dependence of ξ_+ on D can be obtained by examining the flow in the vicinity of the minimum of the curve at $K^{-1}=K_f^{-1}$ (see Fig. 7). Let $X=K^{-1}-K_f^{-1}$ be the distance from the minimum. Generically, for small X, we have

$$Y^2=\lambda X^2+D, \tag{5.16}$$

where λ is proportional to the curvature at the minimum. It is easy to check that, in this case, the coefficient of Y on the right-hand side of either Eq. (5.12c) or (5.13c), whichever applies, is linearly proportional to X. Using (5.16), we can write the flow equation for Y as

$$dY/dl=\gamma^{-1}(Y^2-D)^{1/2}Y, \tag{5.17}$$

where γ is a nonuniversal number which depends on the location of the fixed point. The parameters D and γ can be scaled away using the substitution $Y\to D^{1/2}Y$ and $l\to\gamma D^{-1/2}l$. This yields a correlation length

$$\xi_+=a\exp(l_+)\simeq a\exp(\gamma/D^{1/2}). \tag{5.18}$$

The dependence of D on the shift of the bare parameters from their critical values can be obtained by solving (5.14) and (5.15).

There is, however, a special case where the curvature of the curve at the minimum vanishes, invalidating the above analysis. This happens at the point S (and correspondingly S') in Fig. 6, where the T_* line meets the phase boundary. The minimum of the curve shown in Fig. 7 is now at the meeting point of the high- and low-temperature segments. This is also the inflection point of each of the two curves. The flow trajectory around the minimum now takes the form

$$Y^2=\tilde{\lambda}|X|^3+D, \tag{5.19}$$

where $\tilde{\lambda}$ is another constant. The flow rate of Y is now proportional to X^2Y. Consequently, we have

$$dY/dl=\tilde{\gamma}^{-1}(Y^2-D)^{2/3}Y, \tag{5.20}$$

where $\tilde{\gamma}$ is yet another number. The proper scaling in this case is $Y\to D^{1/2}Y$ and $l\to\tilde{\gamma}D^{-2/3}l$. A new dependence of the correlation length on D follows,

$$\xi_+\simeq a\exp(\tilde{\gamma}/D^{2/3}). \tag{5.21}$$

4. Free energy

Let us now turn to the behavior of the free energy in the vicinity of the transition. Following the discussion of Sec. IV A, we may write the contribution to the free energy per unit area from pairs in the size range R to $R+dR$ as

$$dF_v\simeq -T\langle\ln(1+y_pz_p)\rangle/R^2. \tag{5.22}$$

Comparing the above equation with (4.5), we obtain

$$y_p\frac{\partial(dF_v)}{\partial y_p}=-T\langle W\rangle/R^2. \tag{5.23}$$

By making analogy to Eqs. (4.17) and (4.19), and using the definition of Y, we find

$$\frac{dF_v}{d\ln R}\simeq\begin{cases}-2\pi TY^2/R^2 & \text{for } T>T_*,\\ -2\pi T_*Y^2/R^2 & \text{for } T<T_*.\end{cases} \tag{5.24}$$

The total vortex contribution F_v to the free energy density of the XY model is obtained by integrating dF_v over R. Let $F_{v,c}$ be the vortex free energy density at the transition. Equation (5.24) then yields

$$F_v-F_{v,c}\sim-\int_a^\infty R^{-3}dR(Y^2-Y_c^2), \tag{5.25}$$

where $Y_c(R)$ is the value of $Y(R)$ at the transition. A full analysis of the integral is quite involved, but the following consideration should yield a correct estimate of the expected singular behavior.

Approaching the transition from the ordered phase, Y flows to 0 at $R=\infty$. The difference $Y^2(R)-Y_c^2(R)$ is expected to remain constant, say, equal to $D<0$, up to $R=\xi_-$, and then goes to 0. Truncating the integral at $R=\xi_-$, we obtain

$$F_{v,-}-F_{v,c}\sim -Da^{-2}+D\xi_-^{-2}. \tag{5.26}$$

The crossover length ξ_- has the same behavior as ξ_+, except that one should replace D by $-D$ in Eqs. (5.18) and (5.21), as the case may be. From the disordered side, the story is the same up to $R=\xi_+$, but beyond that Y^2 becomes of order 1. Hence we expect

$$F_{v,+}-F_{v,c}\sim -Da^{-2}-\xi_+^{-2}. \tag{5.27}$$

The singularity of $F_{v,\pm}$ is thus related to the singular behavior of $\xi_\pm$. In both cases, it is an essential singularity.

Finally, it is interesting to see if the pair-freezing line T_* in the ordered phase corresponds to another singularity of the vortex free energy. The analysis presented in Appendix D suggests that this is not the case. We should, however, note that the absence of a true glass transition in our model is a result of the very special type of functional dependence of relevant quantities on temperature and pair size, and hence might be susceptible to various types of perturbations.

C. Two-point correlation function

Consider now the two-point phase-phase correlation function

$$C(r_{ij}) \equiv \langle \exp[i(\phi_i - \phi_j)] \rangle, \tag{5.28}$$

where the average is taken over thermal and then disorder fluctuations. When only spin-wave contributions to ϕ are taken into account, one obtains a power-law decay of C with distance r_{ij}, as shown in Eq. (1.3). Vortex-pair excitations ''soften'' the spin waves, and lead to a faster decay of the correlation function. On grounds of the renormalizability of the model, one expects that, in the ordered phase,

$$C(r) \sim r^{-\eta} \tag{5.29}$$

at large distances, but the exponent η differs from $\eta_{\rm sw}$ in that the renormalized values K_∞^{-1} and σ_∞ should be used,

$$\eta = \frac{1}{2\pi}(K_\infty^{-1} + \sigma_\infty). \tag{5.30}$$

The above conjecture for the average behavior of $C(r)$ can be verified by a direct calculation. Since the spin-wave and vortex fluctuations decouple, and the disorder which enters $H_{\rm sw}$ is orthogonal to the disorder in H_v (see Sec. II A), we may write

$$C(r) = C_{\rm sw}(r) C_v(r), \tag{5.31}$$

where $C_v(r)$ is the correlation of phases ϕ_v generated by vortex excitations,

$$C_v(r_{ij}) \equiv \langle \exp[i(\phi_{v,i} - \phi_{v,j})] \rangle. \tag{5.32}$$

Following Kosterlitz,[2] we calculate the right-hand side of (5.32) by successive elimination of vortex-antivortex pairs, starting from the smallest pair size. The formula below gives the difference in the phase at two sites i and j, generated by a single vortex-antivortex pair at $\mathbf{r}_p$:

$$\phi_{v,i} - \phi_{v,j} \simeq (2\pi J)^{-1} (\mathbf{p} \times \hat{\mathbf{z}}) \cdot \mathbf{E}(\mathbf{r}_p), \tag{5.33}$$

where $\mathbf{p}$ is the dipole moment of the pair (assumed to have a magnitude R much smaller than r) and $\mathbf{E}(\mathbf{r}_p)$ is the electric field at $\mathbf{r}_p$ due to a $+1$ charge placed at site i and a -1 charge placed at site j. The variance of the phase difference generated by *all pairs* in the size range R to $R+dR$ can now be easily calculated with the help of the equivalence of Eqs. (AQ6) and (A8),

$$\langle (\phi_{v,i} - \phi_{v,j})^2 \rangle_{dR} \simeq 2\pi \langle W \rangle \ln(r_{ij}/R). \tag{5.34}$$

Going from R to $R+dR$, $C_v(r)$ is reduced by a factor

$$\exp[-\tfrac{1}{2} \langle (\phi_{v,i} - \phi_{v,j})^2 \rangle_{dR}] \simeq (r/R)^{-d\eta}. \tag{5.35}$$

Comparing the coefficient of the logarithm in (5.34) with Eqs. (4.9), (4.16), and (5.11), we obtain

$$d\eta = \frac{1}{2\pi}(dK^{-1} + d\sigma), \tag{5.36}$$

which is nothing but the differential form of (1.4). This confirms the intuitive idea that the asymptotic value of η is given by (5.30). On the transition line, η decreases monotonically from the value 1/4 for the pure case to 1/16 at the zero-temperature transition point.[18]

Inspecting Eq. (5.33), we see that spatial and angular localization of the vortex-antivortex pairs may lead to a rare, but significant deviation of the thermally averaged correlation function at two fixed sites i and j,

$$\tilde{C}_v(\mathbf{r}_i, \mathbf{r}_j) \equiv \langle \exp[i(\phi_{v,i} - \phi_{v,j})] \rangle_{\rm thermal}, \tag{5.37}$$

from its average value $C_v(r_{ij})$. Such a fluctuation comes about when we are looking at large-size pairs which have strong density fluctuations (after thermal averaging) on the scale r_{ij}, and that the presence or absence of such a pair in the region surrounding i and j will make a significant change to the phase difference $\phi_{v,i} - \phi_{v,j}$. Below T_*, the typical density of these pairs is significantly smaller than the average density. Consequently, the typical value of the exponent, $\eta_{\rm typ}$, can be somewhat smaller than its average value η.

VI. SUMMARY

The main conclusions of the present work can be summarized as follows. When the variance σ of the random phase shifts is sufficiently small, the quasi-long-range order of the 2D XY model survives at sufficiently low temperatures. The two-point phase-phase correlation decays algebraically with distance in the entire ordered phase up to the transition. At the transition, the exponent of the power-law decay lies in the range between 1/16 and 1/4. Approaching the transition from the disordered side, the correlation length diverges exponentially with a $-\frac{1}{2}$ or $-\frac{2}{3}$ power of the distance from the transition point. The free energy exhibits an essential singularity on the phase boundary. For $\sigma > \sigma_c$, the system is in the paramagnetic phase at any $T > 0$, without a finite-temperature glass transition. The value of σ_c is nonuniversal but should be smaller than $\pi/8$.

The behavior of vortex-antivortex pairs inside the ordered phase is quite interesting. In contrast to the pure case, there is a finite density of such pairs at zero temperature. As the temperature T increases, the pair density increases, initially slowly up to $T = T_*$, and then grows rapidly as entropy comes into play. Following an opposite sequence, as T is lowered from the transition temperature, large-size pairs undergo various degrees of localization both in space and in its angular distribution. However, in the Coulomb gas language, a finite susceptibility for the gas of pairs is found at all temperatures. Localization also introduces a zero-field random polarization of the gas of pairs, which has the effect of enhancing disorder seen by large-size pairs.

Much of the qualitative aspects of our results agree with those of NSKL (Ref. 18) and of Cha and Fertig,[19] though there are minor but important differences on a quantitative level. Technically, the analogy introduced here to the random energy model offers a heuristic understanding of some of the subtle features introduced by the disorder potential, responsible for the failure of previous calculations based on a small-fugacity expansion. In fact, we have shown that an expansion with respect to the pair fugacity y_p fails for any $\sigma > 0$. A somewhat surprising result is that no singularity in the free energy is found at T_*. The whole analytic structure of the free energy as a function of T and σ remains to be explored.

The question of a possible reentrance transition at a disorder strength σ sufficiently close to the critical value σ_c cannot be satisfactorily addressed within the level of accu-

racy of the RG method adopted here. In fact, due to the renormalization of σ we obtained, there is room for the reentrance scenario, though it is clear that reentrance does not occur at weak disorder. In this connection, it would be very interesting to consolidate our work and that of Ozeki and Nishimori[16] on a model which admits gauge symmetry. (See also Ref. 20.)

A new quantity which appeared in this paper is the single-vortex glass temperature T_g. This temperature also signals localization in the angular distribution of a pair when translation of the pair over a distance larger than its size is forbidden. As we have seen, T_g plays no special role in the thermodynamics of the XY model. Nevertheless, one might contemplate possible changes of dynamical behavior at T_g, an issue to be studied further.

ACKNOWLEDGMENTS

During the course of this work, I have benefited greatly from discussions with Bernard Derrida, Sergei Korshunov, Thomas Nattermann, and Stephan Scheidl. Part of the work was done at the Weizmann Institute during a very pleasant workshop organized by Professor David Mukamel and Professor Eytan Domany. Research is supported in part by the German Science Foundation through Project No. SFB-341.

APPENDIX A: ELECTROSTATICS IN TWO DIMENSIONS

In this appendix we collect some useful formula from electrostatics in two dimensions. We adopt the convention that the unit of charge is 1. The electric potential due to a $+1$ charge at origin is given by

$$V(\mathbf{r}) = -\epsilon^{-1}\ln(|\mathbf{r}|/a), \tag{A1}$$

where $\epsilon=(2\pi J)^{-1}$ is the bare dielectric constant. The electric field $\mathbf{E}=-\nabla V$ satisfies

$$\nabla\cdot\mathbf{E}=2\pi\epsilon^{-1}\rho(\mathbf{r}), \tag{A2}$$

where $\rho(\mathbf{r})$ is the charge density at $\mathbf{r}$.

In a dielectric medium, the induced polarization $\mathbf{P}=\chi\mathbf{E}$, where χ is known as the dielectric susceptibility. The displacement vector $\mathbf{D}=\epsilon\mathbf{E}+2\pi\mathbf{P}$ satisfies

$$\nabla\cdot\mathbf{D}=2\pi\rho_f(\mathbf{r}), \tag{A3}$$

where $\rho_f(\mathbf{r})$ is the density of free charges at $\mathbf{r}$. Writing $\mathbf{D}=\tilde{\epsilon}\ \mathbf{E}$, we obtain

$$\tilde{\epsilon}=\epsilon+2\pi\chi. \tag{A4}$$

Let us now consider three examples encountered in the main text. In the first example we establish the equivalence of two expressions for the energy of a charge-neutral system. The electric field generated by a set of point charges m_i located at $\mathbf{r}_i$ is given by

$$\mathbf{E}(\mathbf{r})=2\pi J\sum_i\ m_i\frac{\mathbf{r}-\mathbf{r}_i}{|\mathbf{r}-\mathbf{r}_i|^2}. \tag{A5}$$

Consider now the integral

$$\mathcal{E}=\frac{1}{8\pi^2 J}\int d^2r|\mathbf{E}|^2. \tag{A6}$$

Writing

$$|\mathbf{E}|^2=V\nabla\cdot\mathbf{E}-\nabla\cdot(V\mathbf{E}), \tag{A7}$$

and using the Gauss's theorem and Eq. (A2), we obtain

$$\mathcal{E}=\sum_i\ m_i^2E_c-\pi J\sum_{i\neq j}\ m_im_j\ln(|\mathbf{r}_i-\mathbf{r}_j|/b). \tag{A8}$$

Here

$$E_c=\frac{J}{2}\int_{|\mathbf{r}|<b}d^2r|\mathbf{r}|^{-2} \tag{A9}$$

is the ''core energy'' of a unit charge. [The divergence of (A9) at small distances is cut off by the existence of a lattice.] Note that, in the continuum, b is an arbitrary parameter which does not influence the result (A8).

As the second example we consider an expression for the interaction energy between a set of charges m_i at $\mathbf{r}_i$ and quenched dipoles $\mathbf{q}_j$ at $\mathbf{R}_j$. Let $\mathbf{E}(\mathbf{r})$ be the electric field generated by all the charges, and $\mathbf{E}_d(\mathbf{r})$ be the field due to the dipoles but excluding those within a distance R from $\mathbf{r}$. Consider now the integral

$$\mathcal{E}_1=\frac{1}{4\pi^2 J}\int d^2r\mathbf{E}\cdot\mathbf{E}_d. \tag{A10}$$

We now write $\mathbf{E}_d$ as a sum over the field due to individual dipoles. Using again (A7) and the Gauss's theorem separately for each j, we obtain

$$\mathcal{E}_1=\sum_i\ m_iV_d(\mathbf{r}_i)+\sum_j\ U_j. \tag{A11}$$

Here $V_d(\mathbf{r})$ is the potential due to dipoles outside a circle of radius R centered at $\mathbf{r}$, and

$$U_j=\frac{1}{2\pi}\int_0^{2\pi}d\phi\mathbf{R}\cdot\mathbf{E}(\mathbf{R}_j+\mathbf{R})\frac{\mathbf{q}_j\cdot\mathbf{R}}{R^2}, \tag{A12}$$

where $\mathbf{R}=R(\cos\phi,\sin\phi)$. Elementary calculation yields $U_j=\frac{1}{2}\mathbf{q}_j\cdot\mathbf{E}(\mathbf{R}_j)$. It follows that the second sum on the right-hand side of (A11) is $-\frac{1}{2}$ times the first sum. Hence

$$\mathcal{E}_1=\frac{1}{2}\sum_i\ m_iV_d(\mathbf{r}_i). \tag{A13}$$

Our final example concerns the field $\mathbf{E}_Q$ inside a circle of radius R generated by a medium with a permanent polarization $\mathbf{Q}$ which fills the circle. To bypass an explicit calculation, we use the result that, in a uniform external field $\mathbf{E}_0$, the field inside such a circle filled with a *polarizable* medium of dielectric constant ϵ_1 is given by

$$\mathbf{E}_1=\frac{2\epsilon}{\epsilon+\epsilon_1}\mathbf{E}_0, \tag{A14}$$

where ϵ is the dielectric constant of the medium outside the circle. The polarization inside the circle is

$\mathbf{Q}=(\epsilon_1-\epsilon)\mathbf{E}_1/(2\pi)$, and the field it produces is $\mathbf{E}_Q=\mathbf{E}_1-\mathbf{E}_0$. Using the above results, we obtain

$$\mathbf{E}_Q=-(\pi/\epsilon)\mathbf{Q}=-2\pi^2 J\mathbf{Q}, \tag{A15}$$

which is uniform inside the circle.

APPENDIX B: FREEZING AND LONG TAILS IN THE RANDOM ENERGY MODEL

As shown by Derrida,[23] the freezing transition in the random energy model can be understood as a switching of terms which contribute most to the partition sum (3.4). For $T<T_g$, the lowest of the N energies x_i dominates z, while for $T>T_g$, typically a finite fraction of the N energies contribute significantly to z. (The word ''typical'' refers to events which occur with a large probability, and ''rare'' refers to events with a very small probability.) This can be seen more explicitly as follows.

In a given realization of the disorder, the random energies fall into a band $x_{\min}\leqslant x_i\leqslant x_{\max}$, where $x_{\min}=\min_i\{x_i\}$ and $x_{\max}=\max_i\{x_i\}$. Introducing the integrated density of state, $\mathcal{N}(x)$, which gives the number of levels with $x_i\leqslant x$, one can rewrite Eq. (3.4) as

$$z=\exp(-x_{\min}/T)+\int_{x_{\min}}^{\infty}\exp(-x/T)d\mathcal{N}. \tag{B1}$$

The contribution from the lowest-energy level has been isolated from the rest. When the total number of levels is large, there are typically many levels in an interval $dx\sim T$, so that one may replace $d\mathcal{N}$ by its mean,

$$d\mathcal{N}\simeq N\psi(x)dx. \tag{B2}$$

Equation (B2) fails when $\mathcal{N}(x)\sim 1$. This happens for $x<x_0$, where x_0 is determined by the condition $\mathcal{N}(x_0)=1$. From Eqs. (B2) and (3.5) we get

$$x_0=-(2s)^{1/2}\ln N+O(\ln\ln N). \tag{B3}$$

Substituting (B2) into (B1), and restricting the integral to $x>x_0$, we obtain

$$z\simeq\exp(-x_{\min}/T)+z_{\text{typ}}, \tag{B4}$$

where

$$z_{\text{typ}}=N\int_{x_0}^{\infty}dx\,\psi(x)\exp(-x/T). \tag{B5}$$

It is easy to show that the typical value of $x_{\min}$ is given by x_0, while the typical value of the partition function is given by

$$z_{\text{typ}}\simeq\exp(-\langle f\rangle/T). \tag{B6}$$

Thus the contribution from the lowest-energy level to z becomes significant in a *typical* realization of the disorder only when $T\leqslant T_g$.

On the other hand, fluctuations of z far away from z_{typ} (say, $z>2z_{\text{typ}}$) are dominated by fluctuations of $x_{\min}$ at all temperatures. This is especially so for $T<T_g$, where the fluctuations of z are typically of order z_{typ}. To characterize this behavior more precisely, let us consider the distribution of $x_{\min}$, denoted by $\psi_{\min}(x)$. For the minimum of the N energies to be greater than a certain number x, all N energies must be greater than x. Hence we have

$$\int_x^{\infty}dy\,\psi_{\min}(y)=\left[\int_x^{\infty}\psi(y)dy\right]^N. \tag{B7}$$

For $x\ll-\sqrt{\Delta}$, the integral on the right-hand side is very close to 1, in which case one can write

$$\psi_{\min}(x)=-\frac{d}{dx}\exp\left[-N\int_{-\infty}^{x}\psi(y)dy\right]. \tag{B8}$$

For $x<x_0$, the argument of the exponential is less than 1, and hence

$$\psi_{\min}(x)\simeq N\psi(x)=\frac{1}{\sqrt{2\pi\Delta}}\exp\left[\left(1-\frac{x^2}{x_0^2}\right)\ln N\right]. \tag{B9}$$

The distribution of $x_{\min}$ gives us an idea about the high end of the distribution of the partition function z, where we can write $z\simeq\exp(-x_{\min}/T)$. On a log-log plot, the local slope of the distribution is essentially given by

$$\zeta(z)=\frac{d\ln\psi_{\min}}{d\ln z}\simeq\frac{T}{T_g}\frac{T\ln z}{x_0}, \tag{B10}$$

which is a slow-varying function of z. This implies that the distribution of z has a long tail. High moments of z are sensitive to the tail of the distribution. Using (B9), we find

$$\frac{\langle z^n\rangle}{\langle z\rangle^n}\simeq\begin{cases}1 & \text{for } T>T_n,\\ N^{(n-1)[(T_n/T)^2-1]} & \text{for } T<T_n,\end{cases} \tag{B11}$$

where

$$T_n=n^{1/2}T_g. \tag{B12}$$

The result agrees with an exact calculation by Derrida starting from (3.4).

APPENDIX C: MEAN PAIR DENSITY AND FLUCTUATIONS

The disorder average of the cell occupation number W can be calculated by expanding Eq. (4.5) as a power series of y_pz_p for $y_pz_p<1$, and a power series of $(y_pz_p)^{-1}$ for $y_pz_p>1$. Denoting by $P(z)$ the probability distribution of z_p, we obtain

$$\langle W\rangle=\sum_{n=1}^{\infty}(-1)^{n-1}I_1(n)+\sum_{n=0}^{\infty}(-1)^nI_2(n), \tag{C1}$$

where

$$I_1(n)=y_p^n\int_0^{1/y_p}z^nP(z)dz, \tag{C2}$$

$$I_2(n)=y_p^{-n}\int_{1/y_p}^{\infty}z^{-n}P(z)dz. \tag{C3}$$

In principle, evaluation of the integrals I_1 and I_2 requires full knowledge of $P(z)$, which we do not have at hand. On the other hand, as we discussed in Appendix B, the large-z tail of $P(z)$ is due to fluctuations of the minimum energy $x_{\min}$. Thus for large z the substitution

$$P(z)dz \to \psi_{\min}(x)dx \simeq N\psi(x)dx, \tag{C4}$$

with $z=\exp(-x/T)$, yields a good approximation. The integral I_2 is now readily calculated. The result reads

$$I_2(n) \simeq \frac{N}{2} y_p^{-n} \exp\left(\frac{n^2\Delta}{2T^2}\right)\left[1-\mathrm{erf}\left(\left(\frac{n}{T}+\frac{1}{T_*}\right)\sqrt{\frac{\Delta}{2}}\right)\right], \tag{C5}$$

where $\mathrm{erf}(u)=2\pi^{-1/2}\int_0^u \exp(-x^2)dx$ is the error function. Here

$$T_* \equiv -\Delta/(T \ln y_p), \tag{C6}$$

which coincides with (1.5) in the limit $R\to\infty$.

The integral $I_1(n)$ can be written as

$$I_1(n) = y_p^n \langle z^n \rangle - I_2(-n). \tag{C7}$$

To obtain its leading-order behavior, we need to examine which part of the distribution $P(z)$ contributes most to the average $\langle z^n \rangle$. For $T>T_n=n^{1/2}T_g$, the main contribution comes from the central part of $P(z)$ around $z_{p,\mathrm{typ}}$, so that

$$I_1(n) \simeq (y_p \langle z_p \rangle)^n. \tag{C8}$$

For $T<T_n$ and $T<nT_*$, the main contribution comes from the tail of $P(z)$ at $z>y_p^{-1}$. In this case, the two terms on the right-hand side of (C7) almost cancel each other. The main contribution to I_1 thus comes from $P(z)$ around $z=y_p^{-1}$, where again the approximate expression for the tail of $P(z)$ can be used. This yields

$$I_1(n) \simeq \frac{N}{2} y_p^n \exp\left(\frac{n^2\Delta}{2T^2}\right)\left[1-\mathrm{erf}\left(\left(\frac{n}{T}-\frac{1}{T_*}\right)\sqrt{\frac{\Delta}{2}}\right)\right]. \tag{C9}$$

When $T_n<nT_*$, the leading-order behavior switches from (C8) to (C9) at T_n, though (C9) appears as a subleading-order term in the temperature range $T_n<T<nT_*$. (This is due to the fact that, around $T=T_n$, $\langle z^n \rangle$ picks up significant contributions from $z\simeq z_{p,\mathrm{typ}}$ and from the tail at $z>y_p^{-1}$.) On the other hand, when $T_n>nT_*$, there is an intermediate-temperature range $nT_*<T<T_n$ where I_1 is dominated by contributions from z between $z_{p,\mathrm{typ}}$ and y_p^{-1}. In this case, $I_1(n)\simeq y_p^n\langle z^n \rangle$, which essentially coincides with the expression (C9). For $n=1$, (C9) is valid at all temperatures.

A careful analysis of the above expressions is quite cumbersome, but the following observations are useful and suffice for our purpose.

(i) Leading-order behavior. For $T>T_*$, $\langle W \rangle$ is dominated by $I_1(1)$,

$$\langle W \rangle \simeq N y_p \exp(\Delta/2T^2). \tag{C10}$$

In terms of parameters of the model, we have

$$\langle W \rangle \simeq 2\pi \exp\left(-\frac{2E_c}{T}\right)\left(\frac{R}{a}\right)^{4-2\pi K+2\pi\sigma K^2}\frac{dR}{R}. \tag{C11}$$

For $T<T_*$, $I_1(n)$ and $I_2(n)$ all contribute. Using the asymptotic expression $\mathrm{erf}(u)\simeq 1-\pi^{-1/2}u^{-1}\exp(-u^2)$ at large u, we obtain

$$\langle W \rangle \simeq A\left(\frac{T}{T_*}\right)\frac{NT_*}{(2\pi\Delta)^{1/2}}\exp(-\Delta/2T_*^2) \tag{C12}$$

or, more explicitly,

$$\langle W \rangle \simeq A\left(\frac{T}{T_*}\right)\left(\frac{2\sigma}{\ln(R/a)}\right)^{1/2}\left(\frac{R}{a}\right)^{4-\pi/(2\sigma)}\frac{dR}{R}. \tag{C13}$$

Here

$$A(u) = u\sum_{n=-\infty}^{\infty}\frac{(-1)^n}{n+u} = \frac{\pi u}{\sin(\pi u)}. \tag{C14}$$

The crossover from (C10) to (C12) is not sharp, but occurs over a temperature range of order

$$\delta T \sim T_*[\sigma/\ln(R/a)]^{1/2}. \tag{C15}$$

[The apparent divergence of $A(T/T_*)$ at $T=T_*$ can be removed by separating out the contribution from $I_1(1)$. This procedure yields a full description of the crossover, which we shall not elaborate here.] Note also that, since $A(0)=1$, $\langle W \rangle$ has a finite value at $T=0$, proportional to the density of cells with a negative ground-state pair energy. For small T, the excess density increases as T^2.

(ii) Correction to the leading-order behavior. For $T>T_*$, the right-hand side of Eq. (C12) appears as a correction to the leading-order behavior, Eq. (C10). The divergence of $A(T/T_*)$ at $T=nT_*$ signals switching of behavior for $I_1(n)$, and the corresponding crossover can be analyzed in detail by isolating out the contribution from this term. When the temperature window $2T_*<T<T_2$ exists, there is another correction term to (C10) from $I_1(2)\simeq y_p^2\langle z^2 \rangle \simeq N y_p^2 \exp(2\Delta/T^2)$. All terms other than these two are shown to be of order $\langle W \rangle^2$ or smaller. Since our treatment of the pair-pair interactions is not accurate enough to produce the coefficient of the $\langle W \rangle^2$ term, these high-order corrections will not be considered.

The above analysis shows explicitly that a perturbative calculation of $\langle W \rangle$ in y_p is dangerous at all temperatures. Even for $T>T_*$, one encounters difficulties when the calculation is carried out to sufficiently high orders, though low-order terms are well behaved. Such behavior is typical for a function which has an essential singularity at $y_p=0$.

The calculation of $\langle W^2 \rangle$ can be reduced to the calculation of $\langle W \rangle$ with the help of the identity

$$\langle W^2 \rangle = -y_p^2 \frac{\partial(y_p^{-1}\langle W \rangle)}{\partial y_p}. \tag{C16}$$

The right-hand side of the above equation can be evaluated using Eqs. (C10) and (C12) in respective regimes. For $T<T_*$, the leading-order result is given by (4.10). For $T>T_*$, the leading-order expression of $\langle W \rangle$ is proportional

to y_p and hence does not contribute to $\langle W^2\rangle$. Going back to Eq. (C1), and keeping the lowest nonvanishing terms, we obtain

$$\langle W^2\rangle \simeq I_1(2)+B\left(\frac{T}{T_*}\right)\frac{NT_*}{(2\pi\Delta)^{1/2}}\exp\left(-\frac{\Delta}{2T_*^2}\right), \tag{C17}$$

where $B(u)=(1-u)A(u)+u/(u-2)$. It is seen that, for $T>T_*$, $\langle W^2\rangle$ is smaller than $\langle W\rangle$ by a factor which decreases as a power law of R. Equation (C17) also accounts for the crossover regime around $T=T_*$, and reduces to (4.10) for $T<T_*$.

APPENDIX D: VORTEX FREE ENERGY IN THE ORDERED PHASE

Following the same idea as in the calculation of $\langle W\rangle$ in Appendix C, we may rewrite (5.22) as

$$dF_v \simeq -\frac{T}{R^2}\left(I_3+\sum_{n=1}^{\infty}\frac{(-1)^{n-1}}{n}[I_1(n)+I_2(n)]\right), \tag{D1}$$

where

$$I_3=\int_{1/y_p}^{\infty}(\ln y_p+\ln z)P(z)dz. \tag{D2}$$

The discussion of Appendix C indicates that a possible source of singularity comes from the terms $I_1(n)$ at $T=T_n$, where the argument of the error function in Eq. (C9) undergoes relatively rapid change. A true singularity, however, appears only in the limit $R\to\infty$. Since the statistical weight of large pairs vanishes rapidly with R, the rapid change of $I_1(n)$ at large R may not produce a singularity in F_v. The following calculation supports this idea.

In terms of $l=\ln(R/a)$, Eq. (C9) can be expressed as

$$I_1(n)=\pi y_p^n \exp(-\theta_n l)[1-\mathrm{erf}(\delta_n l^{1/2})]dl, \tag{D3}$$

where

$$\theta_n=2\pi nK-4-2\pi\sigma n^2K^2, \tag{D4}$$

$$\delta_n=2nT_g/T-2T_g/T_*. \tag{D5}$$

Substituting (D3) into (D1), and integrating over l, we obtain the contribution to F_v from $I_1(n)$,

$$F_{v,1}(n)\simeq(-1)^n y_p^n\left(\frac{\pi T}{na^2}\right)\frac{[\pi/(2\sigma)-2]^{-1/2}}{\delta_n+[\pi/(2\sigma)-2]^{1/2}}. \tag{D6}$$

In deriving the above equation, we have neglected a weak dependence of the parameters σ and $K=J/T$ on R, which is justified asymptotically in the ordered phase. It is clear from (D6) that the free energy has no singularity at $\delta_n=0$ or any other point in the ordered phase for any n.

[1] J. M. Kosterlitz and D. J. Thouless, J. Phys. C **6**, 1181 (1973).
[2] J. M. Kosterlitz, J. Phys. C **7**, 1046 (1974).
[3] V. L. Berezinskii, Zh. Éksp. Teor. Fiz. **61**, 1144 (1971) [Sov. Phys. JETP **34**, 610 (1972)].
[4] D. R. Nelson, in *Phase Transitions and Critical Phenomena*, edited by C. Domb and J. Lebowitz (Academic Press, London, 1983), Vol. 7; P. Minnhagen, Rev. Mod. Phys. **59**, 1001 (1987), and references therein.
[5] M. Rubinstein, B. Shraiman, and D. R. Nelson, Phys. Rev. B **27**, 1800 (1983).
[6] R. F. Voss and R. A. Webb, Phys. Rev. B **25**, 3446 (1982); R. A. Webb, R. F. Voss, G. Grinstein, and P. M. Horn, Phys. Rev. Lett. **51**, 690 (1983); S. Teitel and C. Jayaprakash, *ibid.* **51**, 1999 (1983).
[7] E. Granato and J. M. Kosterlitz, Phys. Rev. B **33**, 6533 (1986); Phys. Rev. Lett. **62**, 823 (1989).
[8] M. G. Forrester, H. J. Lee, M. Tinkham, and C. J. Lobb, Phys. Rev. B **37**, 5966 (1988); S. P. Benz, M. G. Forrester, M. Tinkham, and C. J. Lobb, *ibid.* **38**, 2869 (1988).
[9] A. Chakrabarti and C. Dasgupta, Phys. Rev. B **37**, 7557 (1988).
[10] M. G. Forrester, S. P. Benz, and C. J. Lobb, Phys. Rev. B **41**, 8749 (1990).
[11] Random displacement disorder has the following defining property. When we go around a closed path connecting a set of superconducting grains, the fluctuation in the magnetic flux enclosed has a variance proportional to the length of the path, rather than the area enclosed by the path. In other words, the fluctuation is determined solely by the displacement of the grains on the path. This is precisely the situation described by uncorrelated A_{ij}'s. A different situation arises when there is variation in grain size, in which case the residual Meissner effect leads to correlated A_{ij}'s and a stronger fluctuation in the flux enclosed.
[12] J. L. Cardy and S. Ostlund, Phys. Rev. B **25**, 6899 (1982).
[13] D. R. Nelson, Phys. Rev. B **27**, 2902 (1983).
[14] M. Paczuski and M. Kardar, Phys. Rev. B **43**, 8331 (1991).
[15] D. Munton, J. Stat. Phys. **68**, 1105 (1992).
[16] Y. Ozeki and H. Nishimori, J. Phys. A **26**, 3399 (1993).
[17] S. E. Korshunov, Phys. Rev. B **48**, 1124 (1993).
[18] T. Nattermann, S. Scheidl, S. E. Korshunov, and M. S. Li, J. Phys. (France) I **5**, 565 (1995).
[19] M.-C. Cha and H. A. Fertig, Phys. Rev. Lett. **74**, 4867 (1995).
[20] For a review of additional work see M. J. P. Gingras, in *Magnetic Systems with Competing Interactions*, edited by H. T. Diep (World Scientific, Singapore, 1994).
[21] S. E. Korshunov and T. Nattermann, Phys. Rev. B **53**, 2746 (1996).
[22] S. Scheidl (unpublished).
[23] B. Derrida, Phys. Rev. B **24**, 2613 (1981); B. Derrida and G. Toulouse, J. Phys. (Paris) Lett. **46**, 223 (1985).
[24] B. Derrida and H. Spohn, J. Stat. Phys. **51**, 817 (1988).
[25] M. Cieplak, J. R. Banavar, M. S. Li, and A. Khurana, Phys. Rev. B **45**, 786 (1992).
[26] M. J. P. Gingras, Phys. Rev. B **45**, 7547 (1992).
[27] H. Nishimori and H. Kawamura, J. Phys. Soc. Jpn. **62**, 3266 (1993).
[28] J. Villain, J. Phys. (Paris) **36**, 581 (1975).
[29] J. Cook and B. Derrida, J. Stat. Phys. **63**, 505 (1991).
[30] See, e.g., T. Nattermann and L.-H. Tang, Phys. Rev. A **45**, 7156 (1992).
[31] Equation (5.9) is slightly different from what one gets with a straightforward substitution, but is actually more correct when screening by fellow pairs is taken into account.